HHS Public Access

Author manuscript

Oncogene. Author manuscript; available in PMC 2013 October 04.

Published in final edited form as:

Oncogene. 2013 April 4; 32(14): 1794–1810. doi:10.1038/onc.2012.200.

Basic anatomy and tumor biology of the RPS6KA6 gene that encodes the p90 ribosomal S6 kinase-4

Yuan Sun[1], **Shousong Cao**[2,*], **Min Yang**[1], **Sihong Wu**[1], **Zhe Wang**[1], **Xiukun Lin**[3], **Xiangrang Song**[4], and **D.J. Liao**[1,*]

[1]Hormel Institute, University of Minnesota, Austin, MN 55912, USA

[2]Department of Medicine, Roswell Park Cancer Institute, Buffalo, New York 14263, USA

[3]Institute of Oceanology, Chinese Academy of Sciences, 7 Nanhai Rd, Qingdao, 266071, China

[4]Shandong Provincial Key Laboratory of Radiation Oncology, Shandong Cancer Hospital and Institute, Jinan 250117, China

Abstract

The RPS6KA6 gene encodes the p90 ribosomal S6 kinase-4 (RSK4) that is still largely uncharacterized. In this study we identified a new RSK4 transcription initiation site and several alternative splice sites with a 5'RACE approach. The resulting mRNA variants encompass four possible first start codons. The first 15 nucleotides (nt) of exon 22 in mouse and the penultimate exon in both human (exon 21) and mouse (exon 24) RSK4 underwent alternative splicing, although the penultimate exon deleted variant appeared mainly in cell clines, but not in most normal tissues. Demethylation agent 5-azacytidine inhibited the deletion of the penultimate exon whereas two indolocarbazole-derived inhibitors of cyclin dependent kinase 4 or 6 induced deletion of the first 39 nt from exon 21 of human RSK4. In all human cancer cell lines studied, the 90-kD wild type RSK4 was sparse but, surprisingly, several isoforms at or smaller than 72-kD were expressed as detected by seven different antibodies. On immunoblots, each of these smaller isoforms often appeared as a duplet or triplet and the levels of these isoforms varied greatly among different cell lines and culture conditions. Cyclin D1 inhibited RSK4 expression and serum starvation enhanced the inhibition, whereas c-Myc and RSK4 inhibited cyclin D1. The effects of RSK4 on cell growth, cell death and chemoresponse depended on the mRNA variant or the protein isoform expressed, on the specificity of the cell lines, as well as on the anchorage-dependent or -independent growth conditions and the in vivo situation. Moreover, we also observed that even a given cDNA might be expressed to multiple proteins; therefore, when using a cDNA, one needs to exclude this possibility before attribution of the biological results from the cDNA to the anticipated protein. Collectively, our results suggest that whether RSK4 is oncogenic or tumor suppressive depends on many factors.

[*]**Corresponding authors:** Dr. Shousong Cao, M.D., Department of Medicine, Roswell Park Cancer Institute, Buffalo, New York 14263, USA, shousong.cao@roswellpark.org, Tel: 1-716-845-1638, Dr. D. Joshua Liao, Ph.D., Hormel Institute, University of Minnesota, Austin, MN 55912, USA, djliao@hi.umn.edu, Tel: 1-507-437-9665.

Conflict of interest

The authors declare no conflict of interest.

Introduction

The p90 ribosomal S6 kinases (RSK) are a family of intracellular serine-threonine kinases that are targets of extracellular signal-regulated kinase (ERK).[1] Four RSK members have been identified so far, i.e. RSKs 1, 2, 3 and 4. Differing from other families in the kinase kingdom, RSK proteins contain two kinase domains, one at each end, besides an ERK binding region.[1] The N-terminal kinase domain is responsible for phosphorylation of substrates, whereas the C-terminal kinase domain has, so far, only one known function being to activate its N-terminal kinase.[2] In response to many growth stimuli, ERK activates RSK by phosphorylation at six sites.[3,4] Inactivation of RSK also involves phosphorylation (at Ser737) by its N-terminal kinase domain, but this phosphorylation decreases the RSK-ERK binding and prevents reactivation of RSK after dephosphorylation of the activation sites.[3] A problem is that these pieces of information are obtained from studies only of RSK1 and RSK2; whether they can be applied to RSK3 and RSK4 is unknown. Actually, comparative analyses of RSK members suggest that each may have distinct roles for specifying ERK signals. For instance, RSK1 has limited interaction with identified targets of RSK2; the four RSK genes are expressed in different patterns during late embryonic stages and in adult tissues.[5] RSK2 and RSK4 differ greatly at their N- and C-terminal sequences, suggesting that these two siblings may differ in functions. The RPS6KA2 that encodes RSK3 has been found to be homozygously deleted in some ovarian cancer cell lines and thus may be a tumor suppressor,[6,7] opposite to the oncogenic RSK1 and RSK2.

The human RPS6KA6 gene that encodes RSK4 is localized in the Xq21 chromosomal region and has several single-nucleotide polymorphisms (SNP) in the coding region.[8] Although the initial study using Northern blot approach detected three RSK4 transcripts in human tissues,[8] so far only one mRNA sequence of human RSK4 (hRSK4) has been documented in the NCBI database. Myers et al cloned a mouse RSK4 (mRSK4) cDNA, which has an additional 5' sequence, coding for additional 96 amino acids (aa), that is not present in the hRSK4 or other RSK members of mouse and human origins.[9] This mRSK4 can inhibit the induction of Xbrachyury (a transcription factor) by fibroblast growth factor 8 (FGF8) in one cell *X. laevis* embryo, but this function is lost when the first 96 aa are deleted.[9] Because FGF8 is a critical intermediator of the Ras-ERK signaling in X. Laevis, the mRSK4 with additional 96 aa may be an inhibitor of this signal pathway.

Information on the abundance of RSK4 in various tissues and cell lines is scarce and is quite conflicting. RSK4 protein level in several tumor cell lines has been shown to be very low but the protein is constitutively activated, i.e. being fully phosphorylated, even in serum-starved cells.[10] However, with another antibody, we easily detected RSK4 protein in human breast cancer tissues and cell lines using immunoblotting and immunohistochemical approaches.[11] Niehof and Borlak have reported that the RSK4 mRNA level is high not only in human and rat livers but also in the Caco-2 human colon carcinoma cells.[12] Moreover, Aroclor 1254, a mixture of polychlorinated biphenyls, can induce RSK4 expression in the kidneys of the rats bearing Streptozotocin-induced diabetes.[12] We also observed a marked induction of RSK4 mRNA in c-*myc* transgenic mammary[13] and pancreatic[14] tumors, partly due to transactivation of the RPS6KA6 gene by the c-Myc protein.[15] Therefore, the

RPS6KA6 gene does not seem to be silent and its expression is inducible, although the gene may be aberrantly methylated in some tumors such as endometrial cancer.[16] Whether the RPS6KA6 is mutated or deleted in any cancer is unknown, but deletion of this gene frequently occurs in the patients of X-linked deafness type 3, mental retardation and choroideremia,[8] which indirectly suggests that loss of RSK4 may not be lethal.

In mouse extraembryonic tissues, expression of RSK4 is inversely correlated with the presence of activated ERK.[9] Knockdown of RSK4 by shRNA in human fibroblasts can abolish P53-induced growth arrest and can decrease p21cip1 expression.[17] Therefore, P53 protein can induce p21cip1 to arrest cell growth not only by the well-characterized transactivation but also by recruitment of RSK4 as an intermediator, which is supported by a report that RSK4 can induce senescence via p21cip1.[18] In line with these results that suggest RSK4 as a tumor suppressor, decreased RSK4 mRNA level has been observed in human colon and renal cancers.[19,20] Moreover, we have observed that ectopic expression of RSK4 can inhibit invasion of T47D and MDA-MB231 (MB231) breast cancer cells in culture and inhibit the metastatic ability of MB231 cells in SCID mice.[15] However, we have also observed that RSK4 mRNA and protein levels are higher in about half of the cases of human breast cancer, compared with the adjacent relatively-normal tissue.[11] High RSK4 levels have been shown to render cell lines of melanoma and kidney carcinoma resistant to sunitinib, a protein kinase inhibitor developed as a chemotherapeutic agent.[21] If RSK4 is a tumor suppressor, the high RSK4 level is auspicious for those breast cancer patients, and the aforementioned induction of RSK4 by c-Myc in transgenic mammary and pancreatic tumors[13,14] may be part of the mechanism for c-Myc induced apoptosis since both transgenic tumors are highly apoptotic.[22–24] On the other hand, if RSK4 is oncogenic, induction of RSK4 by c-Myc may be a mechanism for c-Myc-induced cell proliferation, and a high RSK4 level in breast cancer is a bad omen. To disentangle these inconsistencies, in this study we anatomized the human and mouse RSK4 transcripts and characterized RSK4 protein isoforms, followed by studies of their basic functions with emphasis on several parameters of cancer biology. Different types of cancers were targeted, as cancer specificity might account for some inconsistencies.

Results

Alternative initiations of mRSK4 and hRSK4 transcripts

At the time we started to study transcription of RSK4, the first two exons of the hRSK4 mRNA (NM_014496) were thought to be poly-thymine (T) sequences, which are now deleted in the updated version (NM_014496.4). Moreover, the mRSK4 mRNA (NM_025949) encodes an additional 96 aa at the N-terminus[9] as aforementioned. We thus suspected that the 5’-end of the original hRSK4 mRNA might not be correct whereas there should be another mRNA variant of mRSK4 that encodes an open reading frame (ORF) similar to its human counterpart. We therefore determined the 5’-end of RSK4 mRNA. We first performed 5’RACE with RNA from Ela-mycPT1 mouse cells.[25,26] As shown in figure 1 (clone 090), we identified a new transcription initiation site that is localized at the 58th nucleotide (nt) calculated from the end of intron 2 of the updated NM_025949.2 sequence. Using approaches of reverse transcription (RT) and polymerase chain reactions (PCR) with

site-specific primers, we detected this short transcript in all malignant or non-malignant mouse cell lines studied, whereas the long transcript (NM_025949.2) was not detected in most of these cell lines. However, the long transcript was highly expressed in the MMTV-c-*myc* transgenic mammary tumors and the Ela-*myc* transgenic pancreatic tumors, much higher than the abundance in the Ela-mycPT1 cell line that was developed from a transgenic pancreatic tumor (Fig. 2A). Since the elastase-1 (Ela-) gene promoter is inactive in the culture situation, it is possible that expression of the NM_025949.2 mRNA is induced by c-Myc in vivo but is decreased in culture, because the transgene is turned off. Moreover, in a mouse embryo cDNA library, the long transcript was detected much more easily than the short form (Fig. 2B), although it is difficult to assess the ratio of the two in this library because it was subtracted and the primers might have different efficiencies.

With 5'RACE we also cloned the 5'-end of hRSK4 mRNA from L3.6pL human pancreatic cancer cells and identified a new initiation site (my092 in Fig. 1) that is localized at the intron 2, and adds additional 222 nt at the 5'-end, of the NM_014496.4 sequence. This long transcript was detected in many human cancer cell lines and tumor tissues we studied (Fig. 3), although its ratio to the short one (NM_014496.4) is difficult to determine, due to different efficiencies of the primers in PCR.

Alternative splicing of mRSK4 at exons 22 and 24

When we used RT-PCR to amplify a 3' part of the mRSK4 mRNA, we fortuitously found that the PCR products appeared as three bands in agarose gel, with the middle band as the dominant one (Fig. 2C). TOPO or T-A cloning of these bands from 4T1 cells followed by sequencing of many plasmid clones revealed that they were the NM_025949.2 sequence and a splice variant without the first 15 nt of the 77-bp exon 22, as depicted in supplementary figure 1 (S-Fig. 1), which is dubbed as Δ15nt variant. This splice should result in an in-frame deletion of 5 aa at a region close to the Ser737 phosphorylation site that is involved in protein degradation of other RSK members.[4] The middle band is likely to be a heterodimer formed between the two sequences with or without the 15 nt. According to our experience, a heterodimer formed between two similar sequences occurs randomly in PCR and thus may disappear or change its abundance under different PCR conditions in a random manner.[27]

The Δ15nt variant was detected in all the normal or cancerous tissues and cell lines we studied. Some data are presented in figure 2C. The mouse plasmid clone (Clone ID: 30015425) we purchased from Open Biosystems happened to be this Δ15nt variant. To determine the ratio of the two mRNAs in 4T1 cells, we amplified 30 randomly selected plasmid clones with PCR. Visualization of the PCR products in agarose gel revealed that nine clones were the one with the 15 nt (+15nt) that migrated slightly slower on the gel, 18 were the Δ15nt that migrated faster, and the remaining three clones might contain both. Figure 2D shows the PCR results from some plasmid clones. Therefore, the +15nt to Δ15nt ratio is roughly 1:2 [(9+3):(18+3)] in 4T1 cells, indicating that at least in some cells or some situations the Δ15nt is dominant. Actually, in most mouse cell lines we studied, the bottom (faster migrating) band of the triplet was more abundant than the top one. Therefore, the Δ15nt should be considered the wild type (wt) while the NM_025949.2 sequence a minor variant.

Visualization in agarose gel of the RT-PCR products of a different 3'-part from 4T1 and many other mouse cell lines also revealed two bands (Fig. 2E). Cloning and sequencing these bands revealed that the top one that was at the expected molecular mass was the NM_025949.2 sequence whereas the bottom band was a splice variant without the whole 132-bp exon 24, coined herein as ΔE24 variant, which should result in an in-frame deletion of 44 aa from the C-terminus of mRSK4. In a panel of mouse embryonic fibroblasts (MEFs) from normal mice or mice with knockout of the p53, PTEN, RPS6KA3 (RSK2), CCND1 or CDKN2A gene (Fig. 2E), the ΔE24 was always detectable although it was less abundant than the intact form.

Sequence results of RT-PCR products and plasmid clones showed the existence of a variant simultaneously lacking the 15 nt of exon 22 and the whole exon 24 (S-Fig. 1). Thus, there are four different mRNAs, named +15nt+E24, −15nt+E24, +15nt−E24, and −15nt−E24 (Δ15ntΔE24), respectively. To analyze the ratios among the four, we better separated, in agarose gel, the RT-PCR products from RSK2−/−MEF because its total mRSK4 mRNA was at such a low level that allowed a better comparison of molecular weight (Fig. 2E and 2F). The results showed mainly the two 15nt containing variants while the two 15nt-deleted mRNAs were barely detected (Fig. 2F). Of the mouse cell lines or tissues we studied, the RSK2−/−MEF was the only one that showed a decrease in the total mRSK4 mRNA level, hardly expressed the 15nt-deleted variants, and was also the one showing the highest ratio of the −E24 to the +E24 variants. In all other MEFs, the two E24 containing variants were much more abundant than the two sans E24, and of the two without E24, the Δ15ntΔE24 was the dominant one (Fig. 2E). Moreover, expression of the E24 containing variants was slightly increased in the MEFs that lack the p53 alone or together with the MDM2, compared with the wt MEF (Fig. 2E). Lack of one or both alleles of PTEN also slightly increased the levels of the E24 containing variants (Fig. 2E).

mRSK4 was dramatically induced in Ela-*myc* pancreatic tumor tissues, compared with normal pancreas (Fig. 2G), which confirms our previous cDNA microarray data.[14] However, the ΔE24 variants were not detectable in the transgenic mammary or pancreatic tumors (Fig. 2G). Actually, a ΔE24 variant was only detected weakly in the kidney, and not in other organs such as the brain, pancreas and liver from normal mice (Fig. 2G). In contrast, many mouse cancer cell lines express the ΔE24 variants (data not shown).

Our sequence data also identified two new SNPs in several mouse cell lines. One is the G565A that changes aa (R141H) and the other is the T2342C in exon 22 (boxed nt in S-Fig. 1).

Alternative splicing of hRSK4 at intron 1 and exon 21

Using PCR and sequencing approaches, we identified two hRSK4 cDNA variants from a human brain cDNA library (Fig. 3A). One variant has three additional exons derived from intron 1 based on the NM_0144946.4 sequence, which are coined as exons 1B (96 bp), 1C (112 bp) and 1D (110 bp), respectively, to distinguish them from the original 117-bp exon 1 (my111 in S-Fig. 2A and S-Fig. 3), but this variant was not detectable in the human cancer cell lines we studied. The other variant contains only the 110-bp exon 1D (my106 in Fig. 1, S-Fig. 2B and S-Fig. 3), the abundance of which was similar to that of the NM_0144946.4

RNA in the cDNA library (Fig. 3A) but was lower than that of the my092 variant in MCF7 and GI101 breast cancer cells (Fig. 3B) as well as L3.6pL and Colo357 pancreatic cancer cells (Fig. 3C).

Transcripts of hRSK4 also underwent alternative splicing at the 141-bp exon 21, which is the human counterpart of the exon 24 in the mouse, as confirmed by RT-PCR amplification of RNA from several cancer cell lines followed by sequencing the PCR products (Fig. 3D). Lack of this penultimate exon should result in an in-frame deletion of 47 aa from the C-terminus of hRSK4 (S-Fig. 2C). The ratio between the two mRNAs with or without this exon varied greatly among cell lines, as exemplified by the ratios in L3.6pL, Panc28, SK-BR3 and MCF7 cells (Fig. 3D). However, like the ΔE24 in the mouse, the ΔE21 variant was not detectable in most normal human organs, although it might be faintly detectable in the normal liver (Fig. 3E). Moreover, we observed that the liver, kidney, pancreas, testis, prostate and placenta expressed relatively higher levels of hRSK4 mRNA than other tissues (Fig. 3E), which in general dovetails with the original report by Yntema et al.[8]

Although mRSK4 lacks 15 nt in exon 22, we did not detect a similar splicing in its human counterpart, i.e. the 77-bp exon 19 (S-Fig. 2C), in any human cell line or tissue we studied. Comparison of the sequence in the intron-exon boundary around this splice site between the human and mouse shows three mismatched base pairs (bp) within the 15-nt sequence, although the encoded 5 aa only have one mismatch (S-Fig. 2D). It remains unknown whether these sequence differences are reasons for why hRSK4 does not undergo a similar alternative splicing.

Effects of chemicals on RSK4 splicing

In a separate study of cyclin-dependent kinase (CDK) activity, we serendipitously found that treatment of Pan28 and MCF15 cells with an indolocarbazole-derived inhibitor of CDK4 and CDK6, coined as NPCD,[28] induced an alternative deletion of the first 39 nt from exon 21 of hRSK4 (S-Fig. 2C and Fig. 4A), resulting in an in-frame deletion of 13 aa from the C-terminus of hRSK4. This splicing was also observed in MCF15 cells treated with Trib-B, another indolocarbazole-derived compound (Fig. 4A). Interestingly, however, we had never been able to detect this splicing in non-treated Panc28, MCF15 and many other cell lines, indirectly suggesting that it is drug-induced only. Moreover, NPCD slightly increased the level of hRSK4 mRNA as well, as detected by RT-PCR of a region shared by all variants (Fig. 4A, 2nd panel).

Treatment of the MCF15 and MB231 human cells as well as the M8 mouse pancreatic cancer cells[26] with the demethylation agent 5-azacytidine (5-Aza) for one week decreased the levels of the ΔE21 or ΔE24 variants but increased the levels of the intact RSK4 (Fig. 4B, 1st and 2nd panels). 5-Aza had no influence in the splicing at the 15th nt of exon 22 of mRSK4 (Fig. 4B, 3rd panel). The total RSK4 mRNA level was not obviously changed by 5-Aza.

RT-PCR assay showed that treatment of several mouse cell lines with the chemotherapeutic agent cisplatin did not obviously change the ratio of the two mRNAs with, to the two without, the 15nt in exon 22, as exemplified in 4T1 and 4T07 cells (Fig. 4C, left panel).

However, cisplatin not only slightly induced mRSK4 level but also shifted the +E24+15nt to the +E24−15nt variant in 4T1 cells, manifested as a very small decrease in the molecular weight of the top band (Fig. 4C, right panel). Moreover, cisplatin caused deletion of E24 in 4T07 cells and, to a less extent, in NMuMG cells (Fig. 4C, right panel). The mRNA level of mRSK4 was slightly induced in 168FARN and 66C14 but decreased in 67NR cells (Fig. 4C, right panel). Therefore, the effects of cisplatin on mRSK4 RNA level and splicing are cell line specific, i.e. depending on the cellular context. The ensuing effects on the protein level were not determined because few antibodies have been identified to have high affinity to mRSK4 and because mRSK4 is expressed to multiple proteins that have not been characterized (see below).

Bioinformatic analyses of RSK4 ORF

To understand why the RPS6K6A transcripts are initiated from, and spliced at, different sites, we performed bioinformatic analyses of RSK4 variants. Different AUG (ATG in DNA sequence) start codons are identified upstream of the authentic ATG, dubbed as uATGs that initiate upstream ORFs (uORFs). There are also many downstream ATGs that initiate short in-frame ORFs. The results are described in supplementary materials and depicted in S-Fig. 3 and S-Fig. 4.

Multiple RSK4 proteins expressed from a single cDNA

We transfected HEK293T cells with a pMIG-hRSK4 construct, of which ATGβ is the first start codon, and performed western blot assays using the N-terminal N20 and AP7944 as well as the C-terminal C20 and ab57231 antibodies (Fig 5A). As expected, the hSRK4 transfectants showed a strong band between 72 and 100 kD (arrowhead in Fig. 5A). From the name of “p90 ribosomal kinase-4”, this band is assumed to be at 90-kD and to be the wt hRSK4, although the protein initiated from ATGβ (745 aa) should be 83872 Dalton only. This 90-kD protein was basically not detectable in the vector transfectants although a larger amount of protein was loaded as shown in the blot for β-actin (Fig. 5A). Besides the 90-kD protein, hRSK4 transfectants also manifested several smaller bands at about 72, 55 and 48 kD, each of which usually appeared as a duplet or triplet as detected by at least two antibodies. The 72- and 55-kD proteins were always more abundant in the hRSK4 transfectants than in the vector counterparts (Fig. 5A). We conclude that 1) the HEK293T cells hardly express the endogenous 90-kD wt RSK4 and 2) the hRSK4 cDNA is simultaneously expressed to multiple proteins. The AP7944 antibody had poor affinity to the ectopic 90-kD protein but it still had high affinity to the 72- and 55-kD proteins (Fig. 5A). Probably, the ectopic proteins (seen in the hRSK4 transfectants) at about 48-kD were posttranslationally modified differently from their endogenous counterparts (seen in the vector transfectants), since they had different affinities to the same antibodies (Fig. 5A).

We also transfected Hela cells with the hRSK4, the intact mRSK4 or the mouse Δ15ntΔE24 variant cloned in a pcDNA3.1 vector. Western blot assay with the N20 antibody showed that the 90-kD protein was again the dominant one in the hRSK4 cDNA transfected cells but its level was very low in the non-transfected and vector-transfected cells (Fig. 5B). The 48-kD protein was also expressed from the hRSK4 cDNA (Fig. 5B). There were additional bands at about 55 and 135 kD, but whether they were expressed from the hRSK4 cDNA was unclear

because they also appeared in the non-transfected cells (Fig. 5B). The C20 antibody also recognized the 90-kD protein expressed from the hRSK4 cDNA and, with a lower affinity, that from the two mouse constructs (Fig. 5B). In addition, the C20 antibody detected the 72-, 55- and 48-kD proteins expressed from the human and mouse cDNA constructs (Fig. 5B). The C20 antibody also recognized the 135-kD protein, similar to the N20. The Ab42100 N-terminal antibody detected multiple proteins at the 90-, 72-, 55- and 48-kD, but it only had a weak affinity to these proteins expressed from the two mouse constructs. The 135-kD protein seemed to show a reciprocal relationship to the abundance of the 90-kD one as detected by N20 and ab42100 in Hela cells (Fig. 5B) and by AP9744 in HEK293T cells (Fig. 5A). The ab57231 C-terminal antibody and the JS-31 antibody using the whole hRSK4 protein as the immunogen recognized mainly the 90-kD protein and a protein at roughly 37-kD expressed from the hRSK4 cDNA (Fig. 5B), which was also detected by C20 and N20 in HEK293T cells (Fig. 5A).

Of the seven antibodies used (also see below), only ab57231 and JS-31 had high affinity to the 90-kD protein expressed from the two mouse constructs (Fig. 5B). The protein expressed from the intact mRSK4 cDNA migrated slightly slower than that expressed from the human cDNA, whereas the human protein migrated similarly to the Δ15ntΔE24 mouse protein (Fig. 5B). Since ATGβ is the first start codon of the human cDNA that initiates a 745-aa protein, this similarity suggests that the mouse Δ15ntΔE24 construct may be initiated from ATGγ to produce a protein of 732 aa, not from ATGβ to produce an even smaller protein of 712 aa. If so, the intact mouse cDNA may also be translated from ATGγ to produce a 781-aa protein (left table in S-Fig. 4), since both mouse constructs have the same 5' part. However, other situations such as different posttranslational modifications may also affect the migration.

We also performed immunoprecipitation (IP) assay to determine the affinity of the antibodies to the native conformation of the multiple proteins. We transfected MCF15 cells with the intact hRSK4 cDNA and the intact mRSK4 cDNA in the pcDNA3.1 vector. IP of the cell lysates of the transfectants followed by immunoblotting, all with the ab42100 antibody, detected many bands, of which the 90- and 72-kD proteins were in the minority whereas the 135-kD protein was the most abundant, followed by the 55-kD protein (Fig. 5C). These results suggest that ab42100 has low affinity to the native conformation of the 90- and 72-kD proteins but high affinity to the native conformation of the 135- and 55-kD proteins. From the empty vector transfectants, only the 55-, 48- and 33-kD endogenous proteins were pulled down at low abundance. IP with nonspecific immunoglobins and protein A/G-conjugated agarose beads, included as a negative control, also pulled down some smaller proteins with close but not identical molecular weights (Fig. 5C). IP of the same MCF15 cell lysates with ab57231 followed by immunoblotting with C20 antibody also detected multiple proteins expressed from the hRSK4 cDNA, with the 90-kD protein as the dominant one, whereas the endogenous 90-kD protein in the vector transfectants was barely detectable (Fig. 5C). IP with a cocktail of N20, C20, ab42100, ab57231 and AP9744 followed by immunoblotting with JS-31 monoclonal antibody detected the 90- and 55-kD proteins, but whether the 55-kD protein is RSK4 or not is unclear since nonspecific immunoglobins also pull down a protein with similar molecular weight (Fig 5C). We had also performed similar experiments with other different combinations of antibodies for IP and immunoblotting, using lysates from not only MCF15 but also other cell lines. The

results varied among blots but within the range of those shown in figure 5C (data not shown).

Multiple endogenous RSK4 proteins at or smaller than 72 kD

Whether RSK4 is readily detectable at the protein level in different types of cells is not as simple a question as it sounds; actually, it has confused and anguished us for years, largely because multiple proteins were detected. As shown in Fig. 6A, JS-31 antibody identified many proteins at 72, 55, 48 and 33 kD in most of the seven human cancer cell lines on a western blot. A 40-kD protein was also abundantly expressed in some cell lines such as T47D and SKBR3. However, the 90-kD proteins, which appeared as a duplet, were expressed only in some cell lines such as L3.6pL and at such a low abundance that they could be detected only when the blot was slightly overexposed (arrowhead in Fig. 6A). More surprisingly, even in the lysates of AsPC-1 cells transfected with the pMIG-hRSK4 construct, loaded into the gel at a smaller amount of protein as a positive control, the 90-kD protein was hardly detectable while proteins at or smaller than 72-kD were already overexposed (Fig. 6A). The JS-31 antibody again showed high affinity to most of these proteins of the mouse origin as seen in the NMuMG cell line.

Western blot of the above set of cell lysates with ab42100 N-terminal antibody also identified multiple proteins, including those at about 72, 55 and 48 kD (Fig. 6B). Proteins around 90-kD were also detected, sometimes as a duplet, in some cell lines and in the AsPC-1 cells transfected with the hRSK4 cDNA. The levels of these 90-kD proteins were lower than those of the 72-, 55- and 48-kD proteins and seemed to be reciprocal to those of the 135-kD proteins that were the most dominant within each cell line and detected as a duplet (Fig. 6B). However, these endogenous 90-kD proteins were not detected by N20 and C20 antibodies, although N20 and C20 detected bands at 72, 55, 40 and 33 kD, and some of these bands appeared as duplet (Fig 6C and 6D). Western blot assay of four pancreatic cancer cell lines using 2102 N-terminal polyclonal antibody detected the 72- and 55-kD proteins, in addition to a protein at about 100 kD (Fig. 6E). A 90-kD protein appeared only in L3.6pL cells (Fig. 6E).

Verification of multiple RSK4 proteins by shRNA

To determine which one of the multiple bands on immunoblots is RSK4, we transfected HEK293T cells with a pSilencer containing RSK4 shRNA, alone or together with our pMIG-hRSK4 construct. Western blot assay using four different antibodies showed that the shRNA markedly down regulated the 90-kD protein expressed from the hRSK4 cDNA, compared with the cells transfected with the cDNA alone (arrowhead in Fig 7A, lanes 2 *vs* 5). The 48-kD protein that was sensitively detected by JS-31 and ab57231 antibodies was also markedly decreased by the shRNA (Fig. 7A, lanes 2 *vs* 5). The 72- and 55-kD proteins were decreased by the shRNA to a less extent, which was only detected by some of the four antibodies. The proteins around 33-kD were also decreased, as detected by JS-31 and ab57231 (Fig. 7A).

Berns et al once designed five RSK4 shRNAs that have been shown to work efficiently.[17] We transfected HEK293T cells with a mixture of these shRNA constructs together with the

pMIG-hRSK4 cDNA. Western blot assay showed that the 90- and 48-kD proteins again were dramatically down regulated by this shRNA cocktail (Fig. 7B, lanes 3 *vs* 5). The 72- and 55-kD proteins were decreased to a less extent as detected by C20 and ab57231 but not by N20 and JS-31 antibodies (Fig. 7B). Similar studies were also performed not only with Hela and other cell lines but also with transfection with single or different combinations of these five shRNA constructs, all resulting in marked decrease of the 90-kD ectopic protein but again only partial decrease of the proteins at or smaller than 72-kD (data not shown).

Regulation of RSK4 by c-Myc, cyclin D1 and serum

Since we have previously observed that c-Myc induces RSK4,[11,13–15] we wonder whether it also regulates RSK4 splicing. Using a mycER™ system in which mycER fusion protein can be activated by treatment with 4-hydroxytamoxifen (4OHT), as described before,[15] we observed that activation of the mycER induced only the intact RSK4 mRNA in T47D (Fig. 8A) and MB231 (Fig. 8C) cells without induction of the ΔE21 variant, compared with the cells without c-Myc activation by 4OHT. In MCF10 cells, the intact RSK4 was already induced slightly prior to activation by 4OHT (Fig. 8B), likely because the mycER was partly activated by some sex steroids in the culture medium, according to our experience in some cell lines. As described before,[15] transfection of Hela cells with a c-*myc* cDNA in a pcDNA3.1 vector also induced the intact RSK4 (Fig. 8D), but the ΔE21 was not affected. These results dovetail with the observations in figure 2G that the ΔE24 variants were not detectable in c-*myc* transgenic mammary and pancreatic tumors. Moreover, the ratio between the variants with or without the 15 nt in exon 22 of mRSK4 did not show obvious change in these transgenic tumors, compared with normal mammary glands or pancreas from the non-transgenic littermates (data not shown), suggesting that c-Myc does not affect the splicing at this site either.

In mycER™ transfected Hela cells, activated mycER inhibited expression of cyclin D1 (D1) (Fig. 8E), which supports our recent observation that inhibition of D1 by c-Myc also occurs in epithelial cells,[29] not just in fibroblasts as reviewed before.[22,30] At the same time, activation of mycER induced CDK inhibitor p21cip1, compared with the vector-transfected, 4OHT-treated cells (Fig. 8E). On the other hand, transfection of T47D cells with two RSK4 siRNA oligos, which down regulated RSK4, up-regulated D1 mRNA level but down-regulated p21cip1, compared with the transfection with a scrambled siRNA (Fig. 8F). Interestingly, transfection of Hela cells with a hRSK4 cDNA also decreased D1 and increased p21cip1, compared to the transfection with the pMT2 empty vector (Fig. 8E). Conversely, transfection of a D1 cDNA in MB231 and L3.6pL cells, which increased the D1 protein level (data not shown), down regulated the mRNA level of the intact hRSK4, compared to transfection with the empty vector (Fig. 8G). The ΔE21 variant was expressed at a low level in these cell lines and was not affected by D1.

Deprival of MB231 cells from serum for two days did not have evident effect on the putative hRSK4 proteins at 72, 55, 48 and 33 kD detected by four antibodies, compared with the cells maintained in 10% serum (Fig. 9A, lanes 1 *vs* 2). However, these proteins were significantly induced in the serum-deprived MB231 cells that were sorted for D1 or its K112E mutant in a pMIG vector (Fig. 9A, lanes 3 *vs* 4 and lanes 5 *vs* 6). Actually, the D1 or

K112E expressing cells showed a slight decrease in the levels of these proteins even when cultured with 10% serum, compared with the vector counterparts (Fig. 9A, lanes 2 *vs* 4 and 6). Similarly, the effect of withdrawal of MCF7 cells from serum was mild on the levels of the 72-, 55-, 48- and 33-kD proteins, but it was evident in the MCF7 cells that were sorted for the D1 cDNA or its K112E mutant (Fig. 9B, lanes 3 *vs* 4 and 5 *vs* 6). In the presence of 10% serum, D1 and its K112E mutant again inhibited these proteins (Fig 9B, lanes 2 *vs* 4 and 6).

Effects of RSK4 on anchorage-dependent growth and cell death

Transfection of MB231, BxPC3 and Hela cells with the intact mRSK4 or hRSK4 cDNA caused a slight, but statistically significant, decrease in the number of viable cells as determined with an MTT assay, compared to the transfection with the empty pcDNA3.1 vector (Fig. 10A, 10B and 10C). For the mRSK4, this effect was attenuated when exon 24 or the first 15 nt in exon 22 was deleted (Fig. 10A, 10B and 10C). However, transfection with the Δ15ntΔE24 construct increased the number of viable cells, especially in BxPC3 and Hela cells that usually were transfected at a better efficiency (Fig. 10 B and 10C). Compared with the empty vector, the intact mRSK4 in BxPC3 cells did not significantly change cell cycle distribution although G1 fraction seemed to be slightly increased while S and G2-M fractions slightly decreased (table 1). Expression of the intact mRSK4 significantly increased cell death reflected by the sub-G1 fraction (table 1). The Δ15ntΔE24, however, increased the S phase fraction although the decrease in G1 phase did not reach a significant level ($p<0.05$), compared with the empty vector (table 1). Therefore, Δ15ntΔE24-caused increase of viable cells, detected by MTT assay, is attributable to increased cell proliferation, decreased cell death, and likely alleviated G1 arrest as well. We did not transfect mouse constructs to mouse cells because they expressed these variants that complicate the result interpretation.

In AsPC-1 cells sorted for different constructs, the intact hRSK4 and its ΔE21 variant also decreased the number of the viable cells as detected by MTT assay, compared with the empty vector (Fig. 10D). Deprival of AsPC-1 cells from 10% serum in culture caused G1 arrest, manifested as increased G1 but decreased S and G2-M fractions (table 2), which is a well known phenomenon seen in most cell types. Ectopic expression of the intact hRSK4 and the ΔE21 variant prevented this serum-starvation induced G1 arrest, exhibited as a smaller G1 fraction and larger S and G2-M fractions, compared with the corresponding vector expressing cells (table 2). However, in the presence of 10% serum, only the intact hRSK4, but no-longer the ΔE21, could still sustain higher S and G2-M fractions (table 2), suggesting that ΔE21 may require additional growth stimuli from serum for such sustentation. Also as expected, a prolonged serum starvation (comparing days 1 and 2 with days 3 and 4) increased the death of AsPC-1 cells as reflected by a higher Sub-G1 fraction, which was further enhanced by the intact RSK4 and the ΔE21 (table 2).

In L3.6pL cells sorted for different constructs, the intact RSK4 and the ΔE21 had a similar effect on cell cycle distribution to that seen in the AsPC-1 cells but at a smaller extent, because L3.6pL cells had a larger fraction in the S phase in routine culture and were refractory to serum starvation (data not shown). On the other hand, both intact RSK4 and

ΔE21 in L3.6pL cells enhanced cell death induced by serum-deprival compared with the vector counterpart (Supplementary table 2), which was more evident than in AsPC-1 cells (data not shown).

Effects of RSK4 on anchorage-independent and in vivo cell growth

In L3.6pL cells sorted for different constructs, the intact hRSK4 decreased the number of colonies in soft agar, compared with the empty vector (Fig. 11A), similar to what we previously observed in MB231 cells.[15] The ΔE21 variant also, although less effective, decreased the colony number. However, in sorted AsPC-1 cells, the intact hRSK4 increased the number of colonies whereas the ΔE21 lost this function (Fig. 11 A).

Xenograft tumors in SCID mice developed from the L3.6pL cells sorted for the intact hRSK4 grew slower than the vector and the ΔE21 expressing tumors at the last time points, whereas the ΔE21 tumors were not significantly different from the vector tumors (Fig. 11B). Surprisingly, however, the number of cells positive for Ki-67, a marker for proliferating cells, was much smaller in the vector tumors than in the intact hRSK4 tumors and in the ΔE21 tumors, as well as in the ΔE21 tumors than in the intact RSK4 tumors (Fig. 11D and 11E). Histologically, vector tumors encompassed more stromal tissue than the intact hRSK4 and the ΔE21 tumors, whereas the stromal content in the ΔE21 tumors and the intact hRSK4 tumors was similar (Fig. 11E). On the other hand, the ΔE21 tumors contained larger necrotic areas than the vector tumors and the intact hRSK4 tumors (Fig. 11E).

The xenograft tumors of AsPC-1 cells sorted for the intact hRSK4 grew similarly to the vector tumors and both grew significantly faster than the ΔE21 tumors (Fig. 11C). Histologically, AsPC-1 cells formed glandular tumors, although this cell line was established from ascites of a pancreatic cancer patient. The viable cells were located mainly in the outer layer of the intact RSK4 tumors. Discrepantly, the number of Ki-67 positive cells was significantly lower in the intact hRSK4 tumors than in the vector tumors and the ΔE21 tumors (Fig. 11 D and 11E). Moreover, the vector tumors encompassed large necrotic areas, but the necrotic areas were even larger in the intact hRSK4 tumors (Fig. 11E). The ΔE21 tumors were less necrotic than the intact hRSK4 tumors (Fig. 11E). Therefore, although the intact hRSK4 tumors weighed more (Fig. 11C), they actually had fewer proliferating cells but more necrosis (Fig. 11E).

Effects of RSK4 on chemoresponse

Using MTT assay we determined the effects of different RSK4 mRNAs on the response of cancer cells to several chemotherapeutic agents, but we did not observe a general effect. In transfected MCF15 cells, the intact mRSK4 moderately increased the resistance to gemcitabine, compared with the empty vector, but the effect of the Δ15ntΔE24 variant was not significant (Fig. 12A). No significant effects of these two mouse constructs were discerned on the response to other chemotherapeutic agents (Fig. 12A). In the AsPC-1 cells sorted for different constructs, the intact hRSK4 also increased the resistance to the CDK4 inhibitor NPCD, although this compound caused growth inhibition of vector expressing cells (Fig. 12B) as we expected from a previous study.[28] The ΔE21 variant lost this effect (Fig. 12B). On the contrary, in sorted L3.6pL cells, both hRSK4 and the ΔE21 sensitized the cells

to cisplatin and gemcitabine, but not to NPCD (Fig. 12C), as determined by a clonogenic survival assay. However, in xenograft tumor models, only sensitization to cisplatin was observed (Fig. 12D) whereas the effect on gemcitabine was lost (Fig. 12E).

Discussion

In this study we first anatomized RSK4 transcripts with special attention on the initiation sites, splice sites, uORF and downstream in-frame ATGs. We then studied the protein products and the basic biology of this gene on cancer related aspects. Several results oppose our expectations and challenge some basic concepts of biomedical research as discussed below.

One cDNA may be expressed to multiple protein isoforms

So often a western blot assay detects multiple bands, and we subjectively regard those bands at “wrong” molecular weights as “artifacts”, as it gives us a convenient reason to present the expected band only and trash the others, if we do not go further to complain to the company for selling us a “lousy” antibody. This is largely because few details have actually been learned about protein translation. Besides the canonical cap-dependent mechanism of translation initiation,[31] there are many known examples of other mechanisms that involve reinitiation, leaky scanning,[32] IRES (internal ribosome entry site), or CITE (cap-independent translational enhancers).[33] Many genes encompass multiple uATGs and downstream in-frame ATGs, just like RSK4. In some situations, the uATGs control the protein yield via ribosome-stalling[34–36] or mRNA decay,[37] especially in a stressed status.[38–40] Unfortunately, currently we still lack a clean system to study these nontraditional mechanisms, as repeatedly pointed out by Kozak.[41–45]

What surprises us the most is that one single hRSK4 cDNA may be simultaneously expressed to multiple proteins at 90-, 72-, 55- and, in some cells, even 48- and 33-kD, since their levels in the cells that were non-transfected or transfected with the empty vector are much lower (Fig. 5A). These proteins do not seem to derive from alternative splicing because the cDNA is intron-less and because different expression vectors have been used to avoid vector-introduced cryptic splice site as concerned by Kozak.[41–45] Moreover, the same cDNA in different cell lines (HEK293T, Hela and MCF15 cells in Fig. 5) may produce different spectrums of proteins, and the 90-kD protein was not even the dominant one when the cDNA is expressed in AsPC-1 cells (Fig. 6). These results indicate that translation of the transcript from the cDNA is regulated by cellular factors that differ among cell lines. These observations are so fundamental for biomedical research because so often we attribute the biological result from a cDNA to the protein at the anticipated molecular weight without carefully examining whether the cDNA also produces other protein isoforms in the cell line used. Moreover, some of the 72-, 55-, 48- and 33-kD proteins are reactive to both N- and C-terminal antibodies. If some of these proteins are RSK4 isoforms as we tend to believe, then there probably is an unknown mechanism of protein modification that can remove a middle region of a protein, since protein splicing has not been known to occur in multicellular organisms.[46] This intriguing possibility also warrants further exploration.

Cancer cells express multiple RSK4 proteins, but at or smaller than 72 kD

We identified several RSK4 mRNAs that differ at the 5' part and encompass four putative first ATGs (ATGα, β, γ and δ) with different uATGs at their upstream that initiate different uORFs and in-frame ATGs at their downstream. As exemplified by the GCN4 mRNA translation,[47–49] even a three-triplet uORF can regulate translation efficiency.[50,51] Therefore, transcription from different initiation sites may be meaningful, as it provides cells with different uORFs as alternative mechanisms for regulation, likely inhibition,[51] of RSK4 protein translation.

In the NCBI database, the NM_025949.2 mRSK4 utilizes ATGα to produce an 860-aa protein that is calculated as 97480 Dalton, whereas the NM_0144946.4 hRSK4 utilizes ATGβ to produce a 745-aa protein calculated as 83872 Dalton. If the mouse my090 we cloned, which lacks ATGα, is translated from ATGγ, the protein should contain 781 aa and weigh 88303 Dalton (left table in S-Fig. 4). However, if it starts from ATGβ, it would produce a 764-aa protein of 86571 Dalton. Moreover, if in the my106 and my111 human variants the protein is initiated from ATGδ, it should also contain 745 aa but would differ from that initiated from ATGβ by the first 27 aa. In line with these calculations, the dominant protein expressed from our hRSK4 cDNA that starts with ATGβ is about 90-kD on western blot, which is thus considered the wt, intact hRSK4. However, in the cancer cell lines we studied, the dominant endogenous proteins detected by most antibodies are at or smaller than 72-kD. Actually, even in the datasheet of these antibodies, the example proteins are shown at about 72–75 kD (see the corresponding companies' website), much smaller than the above calculations. Therefore, currently we still do not know which ATG is authentic, partly because some posttranslational modifications, besides initiation from a downstream ATG, can also yield smaller proteins. Actually, these smaller proteins may have been subjected to complex posttranslational modifications, as they are often detected as duplet or triplet and show different affinities to different antibodies. What still bewilders us is that all seven RSK4 siRNAs we used can efficiently down regulate the cDNA-derived 90-kD protein but can only partially decrease the 72-kD, 55-kD and some smaller proteins. Unlike the cDNA-derived 90-kD protein, the 72-kD or smaller proteins can be translated from both ectopic and endogenous transcripts that differ at the 5'- and 3'-untranslational regions (UTR). Therefore, the siRNAs may have different efficiencies in demolishing these transcripts or blocking their translation or, conversely, be titrated by separately transcribed 3'-UTR[52,53] from the endogenous allele that remains to be determined.

Of the seven antibodies used, ab42100 and 2102 can detect endogenous proteins at 90-kD in some cancer cell lines, although their expression varies greatly. We tend to consider that these proteins are nonspecific, as most antibodies cannot detect them. The abundance of these 90-kD proteins seems reciprocal to that of the 135-kD proteins which appear as a duplet and are the most dominant among the ab42100 detected proteins (Fig. 6B). These 135-kD proteins may be nonspecific as well, as they are too large and are abundant in Hela cells wherein RSK4 mRNA levels are low (Fig. 3B). However, this conjecture is opposed by the facts that sometimes they are also detected by N20, C20 and JS-31 antibodies. Therefore, their identity remains unknown. Examples for a protein that migrates much more sluggishly

than expected on a western blot include estrogen receptor α, which is 66-kD but could be detected at 116-kD or even 140-kD, due to unknown reasons [54 and references therein].

Unlike all the previous studies that never show or describe RSK4 molecular weight, including those from us, this study shows for the first time the whole immunoblots of different cell lines involving different antibodies. Protein multiplicity and variation overarch these data, even after deducting the possibly nonspecific ones, which may underlie the versatility, flexibility and variety of RSK4's functions as discussed below. While it is difficult to quantify so many bands on immunoblots, these blots actually present the reproducibility at a higher level, compared with repeats, which we actually have, of each blot of the same cell lines and same antibodies. The proteins detected by more antibodies are more likely to be RSK4 isoforms than those appearing on fewer blots. The finding that the endogenous RSK4 proteins in cancer cells are 72-kD and smaller is astonishing, as it implies that not only the previously published data need to be reevaluated accordingly but also studies using cDNA, from which the 90-kD protein is dominant in most cases, should also be interpreted accordingly.

Skip of the penultimate exon may be a feature of an abnormal status

Skip of exon 21 from hRSK4 is observed in MCF10 benign cells and in some cancer cell lines but not in most normal human organs. Similarly, skip of exon 24 from mRSK4 is observed in mouse cancer cell lines and MEF but not in most normal mouse organs, although it is detectable in mouse kidneys. Therefore, deletion of this penultimate exon seems to occur mainly in a non-physiologic status, such as in cell culture or in tumors, which warrants further studies with primary benign and malignant tumor tissues. Even when it is detected, the mRNAs with this exon are still more abundant than those sans it, with the RSK2−/−MEF as an only exception we know, wherein the total RSK4 mRNA level is decreased and the +15nt-E24 variant is dominant (Fig. 2E and 2F), suggesting an interrelationship between these two RSK siblings.

Some chemicals can regulate RSK4 splicing

Demethylation agent 5-Aza can prevent the deletion of the penultimate exon to maintain the intact RSK4 as the dominant one. This may not be due to its demethylation of the RPS6KA6 gene since the total mRNA level of RSK4 is not obviously increased upon the 5-Aza treatment. 5-Aza is known to have many other direct or indirect effects besides DNA demethylation, some of which may contribute to this newly observed regulation of RSK4 splicing.

Somewhat opposite to the effect of 5-Aza, two indolocarbazole-derived CDK4 inhibitory compounds, NPCD and Trib-B, can cause deletion of the first 39 nt from exon 21 of hRSK4. This effect is not universal but rather is site-specific, since deletion of the whole exon 21 or the first 15 nt of exon 19 is unaffected. Identification of splice-regulating compounds is very useful but it is a difficult research area. So far only very few such compounds have been discovered, as reviewed by Sumanasekera et al.[55] Our finding elongates the list of these compounds and may provide a good model for this research area.

Serum, D1 and c-Myc regulate RSK4 and complicate its function

Withdrawal of cells from serum in culture for two days does not obviously induce RSK4 proteins, although the effect may be significant if serum starvation is prolonged. However, serum starvation is additive to increased D1 expression in the induction of the 72-, 55-, 48- and 33-kD, but not the 90-kD, proteins (Fig. 9A and 9B). Many factors in serum promote cell growth in a significant part by activation of D1,[30] and thus may also inhibit RSK4. Therefore, some of the RSK4 protein isoforms may inhibit cell growth while their decreases may facilitate cell proliferation (Fig. 8H). However, the net impact of RSK4, as also discussed below, is more complicated in part because each of the protein isoforms may have different roles. Moreover, since c-Myc induces RSK4 but inhibits D1 whereas RSK4 inhibits D1, inhibition of D1 by c-Myc may be elicited partly via its induction of RSK4 (Fig. 8H). On the other hand, D1 also inhibits RSK4. These complex interactions among these three genes may make RSK4 expression very sensitive to variation in culture condition and to other factors, in turn enlarging the variation in its functions and raising the complexity to a higher level. Unfortunately, our dissection of each isoform's function is hindered by the lack of an RSK4 deficient cell line as a tool and by the situation that a cDNA simultaneously expresses multiple protein isoforms.

As reviewed recently,[30] D1 may regulate transcription of other genes by binding to other proteins without involving CDKs. The K112E mutant of D1 can still bind to, but cannot activate, CDK4 or CDK6.[30] Since decrease of RSK4 by D1 also occurs at the mRNA level (Fig. 8D and 8E) and since K112E can still down regulate RSK4 proteins (Fig. 9A and 9B), this effect of D1 may not require the CDK's kinase activity, which explains why most bands on immunoblots are all decreased while splicing is not affected.

Whether RSK4 is oncogenic or tumor-suppressive depends on many factors

As introduced earlier, available information on the functions of RSK4 is minimal and quite inconsistent. Results from this study provide five possible explanations for the inconsistency: 1) Relative to the empty vector, intact hRSK4 in AsPC-1 cells decreases the number of viable cells in monolayer culture (Fig. 10D), increases the number of colonies in soft agar (Fig. 11A), and decreases the cell proliferation in xenograft tumors as marked with Ki-67 (Fig. 11E). These results suggest that the effects of hRSK4 in a given cell type vary among anchorage-dependent and -independent growth conditions and the in-vivo situation. 2) On the contrary, in L3.6pL cells, the intact hRSK4 decreases the number of colonies in agar (Fig. 11A) but increases the cell proliferation in xenograft tumors (Fig. 11E). The opposing results seen in AsPC-1 and L3.6pL cells suggest that the effects depend on cellular factors that vary among cells. 3) In many cases, deletion of the penultimate exon attenuates the effects of hRSK4, manifested by, e.g., an intermediate number of colonies and Ki-67 positive cells (Fig. 11A and 11E). In the mouse, the Δ15ntΔE24 variant promotes cell growth, opposite to the intact mRSK4. These results indicate that alternative splicing may affect RSK4 functions. 4) Intact hRSK4 inhibits stromal formation in xenograft tumors developed from some cell lines such as L3.6pL but promotes cell death in xenograft tumors developed from some other cell lines such as AsPC-1 (Fig 11E), suggesting that RSK4 may cause cell death in vivo and influence stromal-cancer cell interactions. 5) The RPS6KA6 gene can produce different transcripts from different initiation sites and one form of mRNA

(cDNA) can produce multiple protein isoforms that may differ in functions. In summary, inconsistency may be discerned if we compare different studies without considering these five aspects. A caveat needs to be given that the nomenclature “intact RSK4” used herein is often referred to our cDNA construct, not the 90-kD protein, and its versatility in protein production is probably a reason for the complex variation of our results.

Because the 90-kD protein is skimpy in many cancer cell lines and transfection of cells with RSK4 cDNA inhibits D1 but induces p21cip1 (Fig. 8E), RSK4 might be growth inhibitory and might sensitize cells to chemotherapy. However, chemosensitization is not a general observation in a screening with MTT assay. Since MTT assay detects only viable cells, an effect may not be manifested if RSK4 promotes cell proliferation but meanwhile also sensitizes the cells to a death inducing drug. Nevertheless, in AsPC-1 and MCF15 cells the intact RSK4 slightly increases the resistance to some chemotherapeutic agents, which is attenuated by deletion of the penultimate exon. On the contrary, clonogenic survival assay shows that the intact RSK4 and its ΔE21 sensitize L3.6pL cells to cisplatin and gemcitabine, although only the effect on cisplatin is discerned in a xenograft model. Therefore, the effects of RSK4 and its ΔE21/24 variants on chemotherapy largely depend on the cellular context and experimental conditions.

As recently discussed,[30] anchorage-independent growth is well accepted as an in-vitro criterion for malignant transformation, but this criterion is challenged by the existence of some cell lines that cannot form colonies in agar but are tumorigenic in immunodeficient mice.[56,57] The opposing effects of the intact hRSK4 on the growth of colonies in agar and xenograft tumors in animals (Fig. 11) also question the fidelity of colony formation as an in vitro criterion for a malignant status of cells.

Conclusion

We have identified a new transcription initiation site and several alternative splice sites of the human and mouse RSK4. The resulting mRNA variants encompass four putative first start codons with short uORFs in the upstream and 18–20 in-frame start codons in the downstream. The penultimate exon deleted variant is mainly observed in cell lines, and not in most normal tissues. Demethylation agent 5-Aza can inhibit the deletion of the penultimate exon whereas two indolocarbazole-derived CDK4 inhibitors can induce alternative splicing at the 39th nt of exon 21 in hRSK4. In all human cancer cell lines studied, the 90-kD wt RSK4 was sparse but, surprisingly, several isoforms at or smaller than 72-kD were expressed. Each of these smaller isoforms often appeared as a duplet or triplet and the levels of these isoforms varied greatly among different cell lines and culture conditions. D1 inhibited the expression of RSK4, which was enhanced by serum starvation, whereas c-Myc and RSK4 inhibited D1. The effects of RS4 on cell growth, cell death and chemoresponse depended on the mRNA variant or the protein isoform expressed, on the specificity of the cell lines, as well as on the anchorage-dependent or -independent growth conditions and the in vivo situation. Moreover, we also observed that a given cDNA might be expressed to multiple protein isoforms; therefore, when using a cDNA, we need to exclude this possibility first, before we can attribute the biological results from the cDNA to

the protein at the anticipated molecular weight. Collectively, our results suggest that whether RSK4 is oncogenic or tumor suppressive depends on many factors.

Materials and Methods

Cell lines and cell culture

Cell line information is described in Supplementary information. All the cells were cultured in routine conditions with DMEM containing 5–10% fetal bovine serum (FBS) unless specified.

Construction of cDNA

A hRSK4 cDNA was received from Dr. Frodin which was cloned into a pMT2 retroviral vector and encodes 1–745 amino acids (aa) with an HA tag at the upstream of the ATGβ.[10] The HA tag was removed to build the intact hRSK4, and the exon 21 was further deleted to make the ΔE21 variant. These intact hRSK4 and ΔE21 were inserted into a pcDNA3.1-neo expression vector (www.invitrogen.com) and also a pMIG (MSCV IRES GFP) retroviral vector that contains an IRES-driven green fluorescent protein (GFP) sequence after the insert. A wt cDNA and its K112E mutant[58] of the CCND1 gene that encodes D1, both of which were tagged with a Flag sequence at the N-terminus, were inserted into a pcDNA3.1-neo vector and the pMIG retroviral vector. A full-length mRSK4 cDNA containing ATGα, the first 15 nt of exon 22, and the exon 24 was received from Dr. Myers[9] while another mRSK4 cDNA lacking the first 15 nt of exon 22 was purchased from Open Biosystems (www.openbiosystems.com; clone ID: 30015425). These two mouse cDNAs were reconstructed to build the Δ15nt, ΔE24, and Δ15ntΔE24 variants with deletion of ATGα at the 5' end and deletion of a large part of the 3' untranslated region, while ATGγ was retained.

siRNA and shRNA

Two hRSK4 siRNA oligonucleotides were purchased from Ambion Biosciences (siRNA ID# 134396 and 134397; www.ambion.com) and were shown previously to work efficiently.[15] Based on the siRNA134397 sequence, we also designed a shRNA and cloned it into a pSilencer vector. In addition, we received five shRNA retroviral constructs, a scrambled shRNA construct as control, and the pRISC-STUFFER empty viral vector from Dr. Berns who developed these shRNAs.[17]

Infection and sorting of cells

An Empty pMIG vector and its insert-containing counterparts were packaged in HEK293T cells with helper plasmids. The resultant viruses in culture medium were used to infect the desired cells, followed by fluorescent activating cell sorting (FACS) for GFP with a BD FACSAria™ II Flow Cytometer (BD Biosciences, San Jose, CA) to purify the construct-bearing cells and remove uninfected cells. After one or two passages in culture, the sorted cells were examined under a fluorescent microscope and basically no non-GFP cells were found, confirming the high efficiency of the cell sorting. Although the c-*myc*, D1 and K112E constructs had been used in Dr. Liao's laboratory for years with confirmed expression

efficiency, RT-PCR and western blot assays were performed and high ectopic expression of the c-*myc* and D1 mRNA and protein in the sorted cells were confirmed (data not shown).

Transfection of cells

Details are provided in supplementary materials.

RT-PCR assay

Details are provided in supplementary materials. Hypoxanthine-Guanine Phosphoribosyl Transferase (HPRT) was used as a loading control,[59] because its expression was much lower than the levels of the β-actin and the glyceraldehyde-3-phosphate dehydrogenase (GAPDH) and thus closer to the expression levels of desired genes. Moreover, the β-actin and GAPDH have too many copies of processed pseudogenes in the human and mouse genomes; it cannot be excluded that some of these pseudogenes are expressed in some cell type since most part of the genomes is transcribed.[60]

5'RACE and TOPO or T-A cloning

Total RNA sample from desired cells was used for 5'RACE assays with FirstChoice RLM-RACE Kit (Ambion, Inc; www.ambion.com) by following the manual. The hR199, hR711, hR297, hR445 and hR4R1s primers (supplementary table 1) were used as reverse primers for 5'RACE of RNA from L3.6pL cells or for PCR amplification of a human brain cDNA library. The mF487 and mR711 primers were used for 5'RACE of RNA from 4T1 mouse cells. After the 5'RACE products were fractionized in agarose gel, the desired bands were purified with UltraClean Gel DNA Extraction Kit (ISC BioExpress; www.bioexpress.com) following the manual, or with a simple method we recently established that did not involve a commercial kit.[61] The purified DNA was ligated into a TOPO vector (Invitrogen; www.invitrogen.com) or a pGEM-T Easy Vector (Promega; www.promega.com). RT-PCR products were also cloned in this way.

DNA sequencing and sequence analyses

Details are provided in supplementary materials.

Western blot assay and antibodies

As described before,[62,63] cells lysates were prepared with inhibitors of proteases, kinases and phosphatases and determined for protein concentration. An equal amount of proteins from each sample was fractioned in 8–10% SDS-PAGE and transferred onto a PVDF membrane as described before.[28] Seven RSK4 primary antibodies were used, including N20 (sc-17176; aa 12–100 of hRSK4 as the antigen) goat polyclonal, C20 (sc-17178; aa 650–700 of hRSK4 as the antigen) goat polyclonal, and JS-31 (sc-100424; recombinant whole hRSK4 as the antigen) mouse monoclonal antibodies from Santa Cruz Biotech (www.scbt.com); ab42100 (aa 2–20 of hRSK4 as the antigen) rabbit polyclonal and ab57231 (aa 636–746 of hRSK4 as the antigen) mouse monoclonal antibodies from Abcam (www.abcam.com); 2102 (N-terminus of hRSK4 as the antigen) rabbit polyclonal antibody from EPITOMICS Inc (www.epitomics.com); and AP7944 (N-terminus of hRSK4 as the antigen) rabbit polyclonal antibody from ABGENT Inc (www.ABGENT.com). Rabbit polyclonal D1 (sc-717 and

sc-718) and c-Myc (C19; sc-788) antibodies as well as a mouse monoclonal β-actin antibody (sc-47778) from Santa Cruz Biotech were used for western blots of D1, c-Myc and β-actin proteins, respectively.

IP assay

As described before,[63] protein lysate (400 μg) from each sample was immunoprecipitated in 400 μl lysate buffer containing 0.2 μg indicated RSK4 antibodies at 4°C for 4 hours with rotation. The IP reaction was then added with protein A/G-conjugated agarose beads (15 μl; from Santa Cruz Biotech Inc) and rotated for another 4 hours. The antigen-antibody complexes were spun down and then washed four times with cold lysate buffer. Proper controls included an aliquot of normal immunoglobins from the same species (from Santa Cruz Biotech Inc) to replace the RSK4 antibody in the IP reaction. The pellets were suspended in 30 μl 2×SDS reducing Western blot loading buffer and boiled for 4 minutes. The immunoprecipitates were used in western blot to detect RSK4 with indicated primary antibody.

mycER™ activation

mycER™ is a construct with the ligand binding domain of human estrogen receptor (ER) alpha tagged at the C-terminus of human c-Myc protein. The mycER™ construct or the corresponding empty pBabe retroviral vector was transfected to desired cells followed by activation of the mycER fusion protein by treatment with 150 nM 4-hydroxyltamoxifen (4OHT) as we described before.[15] The cells were harvested 24 hours later for preparation of total RNA samples.

Treatment with chemotherapeutic agents

Indicated cell lines cultured with DMEM containing 5% FBS were treated with 5 μM NPCD or Trib-B, both of which are indolocarbazole analogs synthesized by us and purified with HPLC with over 99% purity.[28] Treatment with DMSO (the solvent) was included as non-treated control. The cells were harvested 3 days later for RT-PCR or 3-(4, 5-Dimethylthiazol-2-yl)-2, 5-diphenyltetrazolium bromide (MTT) assays. Cells treated with 15 μM 5-azacytidine (5-Aza) for one week, with medium change every other day to maintain the drug concentration, were also harvested for RT-PCR. Treatments with other chemotherapeutic agents were the same as described before.[25,26]

MTT assay

Details were described before[28] and in supplementary materials.

Clonogenic survival assay

As described before,[25] cells were seeded in 24-well plates at 1×10^5 cells per well and 24 hours later the desired chemotherapeutic agent was added into the culture, with the same solvent as the non-treated control. Two days later the cells were trypsinized, collected, counted, and then evenly reseeded at 1000 cells per well in triplicate in a 6-well plate. Cells were maintained in culture for 10 to 15 days, with medium change every three days, to let the viable cells propagate to sizable colonies for quantification. The colonies were fixed

with methanol-acetic acid at 3:1 ratio and then stained with 1% crystal violet for 30 minutes. The number of colonies was counted and photographed using Digital Camera.

Anchorage-independent growth assay

Cells harvested from routine culture were suspended in PBS and counted. An equal volume of suspension that contained 1000 cells was mixed with a DMEM containing 0.35% agar and 10% FBS. The mixture was then seeded in each well of a 6-well culture plate that was pre-coated with a layer of basal agar made with 0.5% agar and 10% FBS in DMEM. The agar was then covered with a 10% FBS-containing DMEM and maintained at 37°C, 5% CO_2 for 14 to 20 days with the topping medium refreshed every four days. When the colonies became sizable, the topping medium was discarded and colonies counted under a Leica DM IRB inverted fluorescence microscope using an automatic colony counting system.

Cell-cycle and cell-death analyses

Details were described before[28] and in supplementary materials.

Xenograft tumor model and in vivo drug treatment

L3.6pL and AsPC-1 cells that were sorted with FACS for bearing different constructs were collected from culture and counted. The cells were inoculated subcutaneously at both the left and the right flanks of adult female SCID mice, with 1×10^6 cells for each inoculation. Five animals, in total of 10 tumor xenografts, were used for each cell clone. Once a tumor became palpable, the tumor size was measured with a caliper every day. The animals for study of tumor growth were euthanized 26 days post inoculation. For the chemoresponse study, an L3.6pL derived tumor collected from the above study was sliced to small pieces. One or two pieces, in total of about 35 mg according to our experience, were subcutaneously implanted with a trocar into both the left and the right flanks of a new set of SCID mice. Five animals, in total of 10 tumors, were used for each experimental group. For study on cisplatin, the tumor bearing animals were injected via a tail vein with a single dose (8 mg/kg) 7 days post tumor implantation, with saline as the vehicle control. The tumor sizes were measured daily with a caliper and the animals were euthanized on day 14. For study on gemcitabine, the tumor bearing animals were injected via a tail vein with Gemzar (150 mg/kg) on days 0 (the day of tumor implantation), 7 and 14, and the animals were euthanized on day 16. Tumor weights were calculated from tumor sizes as described previously.[64] All animals were housed in an AAALAC-accredited facility with water and food supplied *ad libitum*. All animal experiments were performed under institutionally approved animal protocols.

Hematoxylin-eosin and Ki-67 staining and quantification

Details are provided in supplementary materials.

Statistical analyses

All MTT, FACS and clonogenic survival assays were performed in multiple repetitions in each experiment, and the experiments were repeated at least three times. Statistical

comparisons between groups were made with the student's t-test or χ square wherever appropriate. The tumor weights, Ki-67 positive indexes, stromal areas and necrotic areas varied greatly and thus analyzed with Wilcoxon rank sum test. All data were presented as mean ± SD (standard deviation). A p value ≤ 0.05 is considered significant in all statistical analyses.

Supplementary Material

Refer to Web version on PubMed Central for supplementary material.

Acknowledgements

This work was supported by a NIH grant RO1 CA100864 and a Pardee Foundation grant on pancreatic cancer to DJ Liao. We would like to thank Dr. Fred Bogott from Austin Medical Center at Austin of Minnesota for his excellent English editing of the manuscript.

References

1. Frodin M, Gammeltoft S. Role and regulation of 90 kDa ribosomal S6 kinase (RSK) in signal transduction. Mol Cell Endocrinol. 1999; 151:65–77. [PubMed: 10411321]
2. Hauge C, Frodin M. RSK and MSK in MAP kinase signalling. J Cell Sci. 2006; 119:3021–3023. [PubMed: 16868029]
3. Dalby KN, Morrice N, Caudwell FB, Avruch J, Cohen P. Identification of regulatory phosphorylation sites in mitogen-activated protein kinase (MAPK)-activated protein kinase-1a/p90rsk that are inducible by MAPK. J Biol Chem. 1998; 273:1496–1505. [PubMed: 9430688]
4. Anjum R, Blenis J. The RSK family of kinases: emerging roles in cellular signalling. Nat Rev Mol Cell Biol. 2008; 9:747–758. [PubMed: 18813292]
5. Kohn M, Hameister H, Vogel M, Kehrer-Sawatzki H. Expression pattern of the Rsk2, Rsk4 and Pdk1 genes during murine embryogenesis. Gene Expr Patterns. 2003; 3:173–177. [PubMed: 12711546]
6. Bignone PA, Lee KY, Liu Y, Emilion G, Finch J, Soosay AE, Charnock FM, Beck S, Dunham I, Mungall AJ, Ganesan TS. RPS6KA2, a putative tumour suppressor gene at 6q27 in sporadic epithelial ovarian cancer. Oncogene. 2007; 26:683–700. [PubMed: 16878154]
7. Lin H, Morin PJ. A novel homozygous deletion at chromosomal band 6q27 in an ovarian cancer cell line delineates the position of a putative tumor suppressor gene. Cancer Lett. 2001; 173:63–70. [PubMed: 11578810]
8. Yntema HG, van den HB, Kissing J, van DG, Poppelaars F, Chelly J, Moraine C, Fryns JP, Hamel BC, Heilbronner H, Pander HJ, Brunner HG, Ropers HH, Cremers FP, van BH. A novel ribosomal S6-kinase (RSK4; RPS6KA6) is commonly deleted in patients with complex X-linked mental retardation. Genomics. 1999; 62:332–343. [PubMed: 10644430]
9. Myers AP, Corson LB, Rossant J, Baker JC. Characterization of mouse Rsk4 as an inhibitor of fibroblast growth factor-RAS-extracellular signal-regulated kinase signaling. Mol Cell Biol. 2004; 24:4255–4266. [PubMed: 15121846]
10. Dummler BA, Hauge C, Silber J, Yntema HG, Kruse LS, Kofoed B, Hemmings BA, Alessi DR, Frodin M. Functional characterization of human RSK4, a new 90-kDa ribosomal S6 kinase, reveals constitutive activation in most cell types. J Biol Chem. 2005; 280:13304–13314. [PubMed: 15632195]
11. Thakur A, Rahman KW, Wu J, Bollig A, Biliran H, Lin X, Nassar H, Grignon DJ, Sarkar FH, Liao JD. Aberrant expression of X-linked genes RbAp46, Rsk4, and Cldn2 in breast cancer. Mol Cancer Res. 2007; 5:171–181. [PubMed: 17314274]
12. Niehof M, Borlak J. RSK4 and PAK5 are novel candidate genes in diabetic rat kidney and brain. Mol Pharmacol. 2005; 67:604–611. [PubMed: 15615695]

13. Thakur A, Xu H, Wang Y, Bollig A, Biliran H, Liao JD. The role of X-linked genes in breast cancer. Breast Cancer Res Treat. 2005; 93:135–143. [PubMed: 16187233]
14. Thakur A, Bollig A, Wu J, Liao DJ. Gene expression profiles in primary pancreatic tumors and metastatic lesions of Ela-c-myc transgenic mice. Mol Cancer. 2008; 7
15. Thakur A, Sun Y, Bollig A, Wu J, Biliran H, Banerjee S, Sarkar FH, Liao DJ. Anti-invasive and antimetastatic activities of ribosomal protein S6 kinase 4 in breast cancer cells. Clin Cancer Res. 2008; 14:4427–4436. [PubMed: 18628456]
16. Dewdney SB, Rimel BJ, Thaker PH, Thompson DM Jr, Schmidt A, Huettner P, Mutch DG, Gao F, Goodfellow PJ. Aberrant methylation of the X-linked ribosomal S6 kinase RPS6KA6 (RSK4) in endometrial cancers. Clin Cancer Res. 2011; 17:2120–2129. [PubMed: 21372219]
17. Berns K, Hijmans EM, Mullenders J, Brummelkamp TR, Velds A, Heimerikx M, Kerkhoven RM, Madiredjo M, Nijkamp W, Weigelt B, Agami R, Ge W, Cavet G, Linsley PS, Beijersbergen RL, Bernards R. A large-scale RNAi screen in human cells identifies new components of the p53 pathway. Nature. 2004; 428:431–437. [PubMed: 15042092]
18. Lopez-Vicente L, Pons B, Coch L, Teixido C, Hernandez-Losa J, Armengol G, Ramon YC. RSK4 inhibition results in bypass of stress-induced and oncogene-induced senescence. Carcinogenesis. 2011; 32:470–476. [PubMed: 21239520]
19. Lopez-Vicente L, Armengol G, Pons B, Coch L, Argelaguet E, Lleonart M, Hernandez-Losa J, de T I, Cajal S. Regulation of replicative and stress-induced senescence by RSK4, which is down-regulated in human tumors. Clin Cancer Res. 2009; 15:4546–4553. [PubMed: 19584160]
20. LLeonart ME, Vidal F, Gallardo D, az-Fuertes M, Rojo F, Cuatrecasas M, Lopez-Vicente L, Kondoh H, Blanco C, Carnero A, Cajal S. New p53 related genes in human tumors: significant downregulation in colon and lung carcinomas. Oncol Rep. 2006; 16:603–608. [PubMed: 16865262]
21. Bender C, Ullrich A. PRKX, TTBK2 and RSK4 expression causes sunitinib resistance in kidney carcinoma- and melanoma cell lines. Int J Cancer. 2011
22. Liao D, Thakur A, Wu J, Biliran H, Sarkar FH. Perspectives on c-Myc, Cyclin D1, and Their Interaction in Cancer Formation, Progression, and Response to Chemotherapy. Crit Rev Oncog. 2007; 13:93–158. [PubMed: 18197790]
23. Liao DJ, Dickson RB. c-Myc in breast cancer. Endocr Relat Cancer. 2000; 7:143–164. [PubMed: 11021963]
24. Liao JD, Adsay NV, Khannani F, Grignon D, Thakur A, Sarkar FH. Histological complexities of pancreatic lesions from transgenic mouse models are consistent with biological and morphological heterogeneity of human pancreatic cancer. Histol Histopathol. 2007; 22:661–676. [PubMed: 17357096]
25. Biliran H Jr, Wang Y, Banerjee S, Xu H, Heng H, Thakur A, Bollig A, Sarkar FH, Liao JD. Overexpression of cyclin D1 promotes tumor cell growth and confers resistance to cisplatin-mediated apoptosis in an elastase-myc transgene-expressing pancreatic tumor cell line. Clin Cancer Res. 2005; 11:6075–6086. [PubMed: 16115953]
26. Biliran H Jr, Banerjee S, Thakur A, Sarkar FH, Bollig A, Ahmed F, Wu J, Sun Y, Liao JD. c-Myc-induced chemosensitization is mediated by suppression of cyclin D1 expression and nuclear factor-kappa B activity in pancreatic cancer cells. Clin Cancer Res. 2007; 13:2811–2821. [PubMed: 17473215]
27. Yang M, Sun Y, Ma L, Wang C, Wu JM, Bi A, Liao DJ. Complex alternative splicing of the smarca2 gene suggests the importance of smarca2-B variants. J Cancer. 2011; 2:386–400. [PubMed: 21811517]
28. Sun Y, Li YX, Wu HJ, Wu SH, Wang YA, Luo DZ, Liao DJ. Effects of an Indolocarbazole-Derived CDK4 Inhibitor on Breast Cancer Cells. J Cancer. 2011; 2:36–51. [PubMed: 21234300]
29. El-Kady A, Sun Y, Li YX, Liao DJ. Cyclin D1 inhibits whereas c-Myc enhances the cytotoxicity of cisplatin in mouse pancreatic cancer cells via regulation of several members of the NF-kappaB and Bcl-2 families. J Carcinog. 2011; 10:24. [PubMed: 22190866]
30. Wang C, Lisanti MP, Liao DJ. Reviewing once more the c-myc and Ras collaboration: converging at the cyclin D1-CDK4 complex and challenging basic concepts of cancer biology. Cell Cycle. 2011; 10:57–67. [PubMed: 21200143]

31. Fitzgerald KD, Semler BL. Bridging IRES elements in mRNAs to the eukaryotic translation apparatus. Biochim Biophys Acta. 2009; 1789:518–528. [PubMed: 19631772]
32. Kozak M. Regulation of translation via mRNA structure in prokaryotes and eukaryotes. Gene. 2005; 361:13–37. [PubMed: 16213112]
33. Shatsky IN, Dmitriev SE, Terenin IM, Andreev DE. Cap- and IRES-independent scanning mechanism of translation initiation as an alternative to the concept of cellular IRESs. Mol Cells. 2010; 30:285–293. [PubMed: 21052925]
34. Iacono M, Mignone F, Pesole G. uAUG and uORFs in human and rodent 5'untranslated mRNAs. Gene. 2005; 349:97–105. [PubMed: 15777708]
35. Ivanov IP, Atkins JF, Michael AJ. A profusion of upstream open reading frame mechanisms in polyamine-responsive translational regulation. Nucleic Acids Res. 2010; 38:353–359. [PubMed: 19920120]
36. Tanner DR, Cariello DA, Woolstenhulme CJ, Broadbent MA, Buskirk AR. Genetic identification of nascent peptides that induce ribosome stalling. J Biol Chem. 2009; 284:34809–34818. [PubMed: 19840930]
37. Nyiko T, Sonkoly B, Merai Z, Benkovics AH, Silhavy D. Plant upstream ORFs can trigger nonsense-mediated mRNA decay in a size-dependent manner. Plant Mol Biol. 2009; 71:367–378. [PubMed: 19653106]
38. Wethmar K, Smink JJ, Leutz A. Upstream open reading frames: molecular switches in (patho)physiology. Bioessays. 2010; 32:885–893. [PubMed: 20726009]
39. Chatterjee S, Pal JK. Role of 5'- and 3'-untranslated regions of mRNAs in human diseases. Biol Cell. 2009; 101:251–262. [PubMed: 19275763]
40. Le Quesne JP, Spriggs KA, Bushell M, Willis AE. Dysregulation of protein synthesis and disease. J Pathol. 2010; 220:140–151. [PubMed: 19827082]
41. Kozak M. Faulty old ideas about translational regulation paved the way for current confusion about how microRNAs function. Gene. 2008; 423:108–115. [PubMed: 18692553]
42. Kozak M. Lessons (not) learned from mistakes about translation. Gene. 2007; 403:194–203. [PubMed: 17888589]
43. Kozak M. Some thoughts about translational regulation: forward and backward glances. J Cell Biochem. 2007; 102:280–290. [PubMed: 17647274]
44. Kozak M. Rethinking some mechanisms invoked to explain translational regulation in eukaryotes. Gene. 2006; 382:1–11. [PubMed: 16859839]
45. Kozak M. A second look at cellular mRNA sequences said to function as internal ribosome entry sites. Nucleic Acids Res. 2005; 33:6593–6602. [PubMed: 16314320]
46. Vila-Perello M, Muir TW. Biological applications of protein splicing. Cell. 2010; 143:191–200. [PubMed: 20946979]
47. Hinnebusch AG. Translational regulation of GCN4 and the general amino acid control of yeast. Annu Rev Microbiol. 2005; 59:407–450. [PubMed: 16153175]
48. Szamecz B, Rutkai E, Cuchalova L, Munzarova V, Herrmannova A, Nielsen KH, Burela L, Hinnebusch AG, Valasek L. eIF3a cooperates with sequences 5' of uORF1 to promote resumption of scanning by post-termination ribosomes for reinitiation on GCN4 mRNA. Genes Dev. 2008; 22:2414–2425. [PubMed: 18765792]
49. Calvo SE, Pagliarini DJ, Mootha VK. Upstream open reading frames cause widespread reduction of protein expression and are polymorphic among humans. Proc Natl Acad Sci U S A. 2009; 106:7507–7512. [PubMed: 19372376]
50. Arava Y, Boas FE, Brown PO, Herschlag D. Dissecting eukaryotic translation and its control by ribosome density mapping. Nucleic Acids Res. 2005; 33:2421–2432. [PubMed: 15860778]
51. Ingolia NT, Ghaemmaghami S, Newman JR, Weissman JS. Genome-wide analysis in vivo of translation with nucleotide resolution using ribosome profiling. Science. 2009; 324:218–223. [PubMed: 19213877]
52. Mercer TR, Wilhelm D, Dinger ME, Solda G, Korbie DJ, Glazov EA, Truong V, Schwenke M, Simons C, Matthaei KI, Saint R, Koopman P, Mattick JS. Expression of distinct RNAs from 3' untranslated regions. Nucleic Acids Res. 2011; 39:2393–2403. [PubMed: 21075793]

53. Salmena L, Poliseno L, Tay Y, Kats L, Pandolfi PP. A ceRNA hypothesis: the Rosetta Stone of a hidden RNA language? Cell. 2011; 146:353–358. [PubMed: 21802130]
54. Liao DZ, Pantazis CG, Hou X, Li SA. Promotion of estrogen-induced mammary gland carcinogenesis by androgen in the male Noble rat: probable mediation by steroid receptors. Carcinogenesis. 1998; 19:2173–2180. [PubMed: 9886575]
55. Sumanasekera C, Watt DS, Stamm S. Substances that can change alternative splice-site selection. Biochem Soc Trans. 2008; 36:483–490. [PubMed: 18481986]
56. Campbell MJ, Wollish WS, Lobo M, Esserman LJ. Epithelial and fibroblast cell lines derived from a spontaneous mammary carcinoma in a MMTV/neu transgenic mouse. In Vitro Cell Dev Biol Anim. 2002; 38:326–333. [PubMed: 12513120]
57. Foster BA, Gingrich JR, Kwon ED, Madias C, Greenberg NM. Characterization of prostatic epithelial cell lines derived from transgenic adenocarcinoma of the mouse prostate (TRAMP) model. Cancer Res. 1997; 57:3325–3330. [PubMed: 9269988]
58. Hinds PW, Dowdy SF, Eaton EN, Arnold A, Weinberg RA. Function of a human cyclin gene as an oncogene. Proc Natl Acad Sci U S A. 1994; 91:709–713. [PubMed: 8290586]
59. Gresner P, Gromadzinska J, Wasowicz W. Reference genes for gene expression studies on non-small cell lung cancer. Acta Biochim Pol. 2009; 56:307–316. [PubMed: 19543558]
60. Palazzo AF, Akef A. Nuclear export as a key arbiter of "mRNA identity" in eukaryotes. Biochim Biophys Acta. 2012
61. Sun Y, Sriramajayam K, Luo D, Liao DJ. A quick, cost-free method of purification of DNA fragments from agarose gel. J Cancer. 2012; 3:93–95. [PubMed: 22359530]
62. Wang Y, Thakur A, Sun Y, Wu J, Biliran H, Bollig A, Liao DJ. Synergistic effect of cyclin D1 and c-Myc leads to more aggressive and invasive mammary tumors in severe combined immunodeficient mice. Cancer Res. 2007; 67:3698–3707. [PubMed: 17440082]
63. Liao DZ, Hou X, Bai S, Li SA, Li JJ. Unusual deregulation of cell cycle components in early and frank estrogen-induced renal neoplasias in the Syrian hamster. Carcinogenesis. 2000; 21:2167–2173. [PubMed: 11133805]
64. Cao S, McGuire JJ, Rustum YM. Antitumor activity of ZD1694 (tomudex) against human head and neck cancer in nude mouse models: role of dosing schedule and plasma thymidine. Clin Cancer Res. 1999; 5:1925–1934. [PubMed: 10430100]
65. Heppner GH, Miller FR, Shekhar PM. Nontransgenic models of breast cancer. Breast Cancer Res. 2000; 2:331–334. [PubMed: 11250725]
66. Shen KC, Miller F, Tait L, Santner SJ, Pauley R, Raz A, Tainsky MA, Brooks SC, Wang YA. Isolation and characterization of a breast progenitor epithelial cell line with robust DNA damage responses. Breast Cancer Res Treat. 2006; 98:357–364. [PubMed: 16541320]
67. Liao DJ, Natarajan G, Deming SL, Jamerson MH, Johnson M, Chepko G, Dickson RB. Cell cycle basis for the onset and progression of c-Myc-induced, TGFalpha-enhanced mouse mammary gland carcinogenesis. Oncogene. 2000; 19:1307–1317. [PubMed: 10713672]
68. Liao DJ, Wang Y, Wu J, Adsay NV, Grignon D, Khanani F, Sarkar FH. Characterization of pancreatic lesions from MT-tgfalpha, Ela-myc and MT-tgfalpha/Ela-myc single and double transgenic mice. J Carcinog. 2006; 5
69. Durnam DM, Palmiter RD. A practical approach for quantitating specific mRNAs by solution hybridization. Anal Biochem. 1983; 131:385–393. [PubMed: 6614474]
70. Liao DJ, Dickson RB. Cell death in MMTV-c-myc transgenic mouse mammary tumors may not be typical apoptosis. Lab Invest. 2003; 83:1437–1449. [PubMed: 14563945]

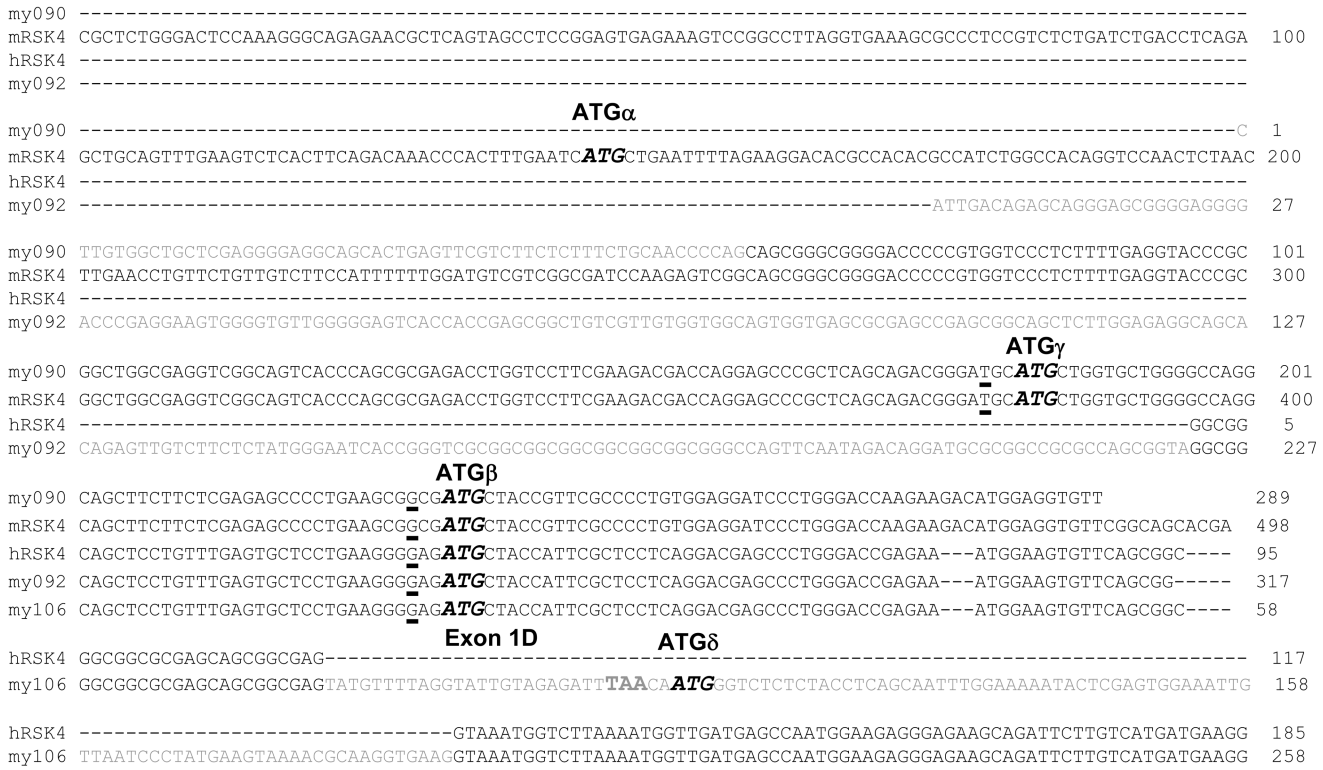

Fig. 1.

Alignment of the NM_025949.2 mRSK4 and the NM_014496.4 hRSK4 as well as the new mouse (my090) and human (my092 and my106) sequences we cloned (grey letters), with the locations of ATGα, β, γ and δ indicated. Note that ATGδ is located in exon 1D, 2 nt downstream of the TAA stop codon of the ORF initiated from ATGβ.

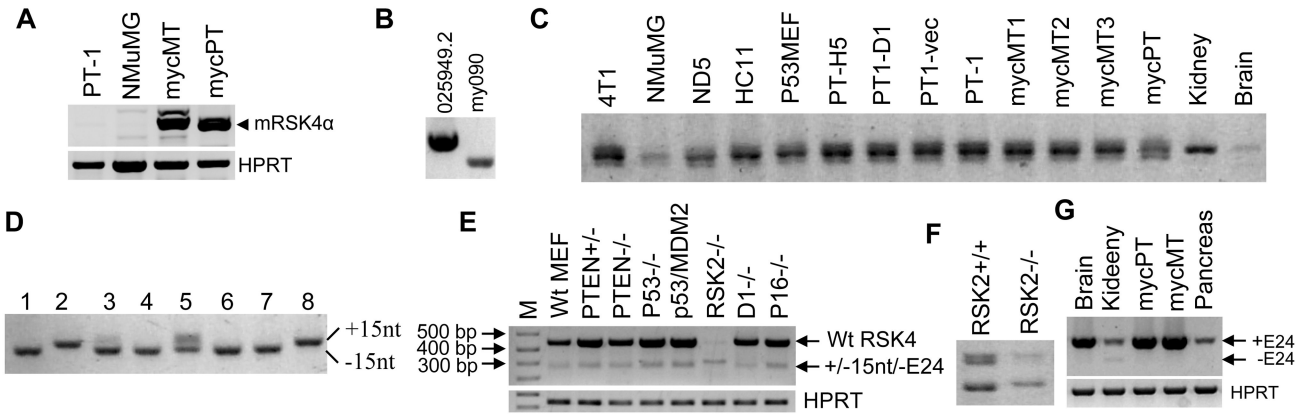

Fig. 2.

RT-PCR detection of splice variants of mRSK4 mRNA. **A**: Detection of the NM_025949.2 mRSK4 initiated from ATGα (mRSK4α) with primers of mF50+mR487 in Ela-mycPT-1 and NMuMG cell lines as well as in one c-*myc* transgenic mammary (mycMT) or pancreatic (mycPT) tumor. HPRT is included as a loading control. **B**: Detection of the long (NM_025949.2) and short (my090) mRSK4 in a mouse embryo cDNA library with a vector primer and mR487. **C**: Detection of the region around exon 22 with primers of mF2155+mR2399 in many mouse cell lines (see supplementary materials) and in mouse tissues of kidney, brain, three c-*myc* mammary tumors (mycMT1, 2 and 3) and one c-*myc* pancreatic tumor (mycPT). Note that the middle band of the triplet, which may be a heterodimer between the +15nt and the −15nt variants, is dominant in all samples. **D**: PCR amplification of eight randomly selected plasmids with primers of mF2155+mR2399 shows that clones 1, 3, 4, 6 and 7 migrate faster and thus are the 15-nt deleted variant, clones 2 and 8 migrate slower and thus are the 15-nt containing variant, whereas clone 5 reveals both bands and may contain both fragments. **E**: Detection of mRSK4 with the mF2155+mR2720 primers in a panel of MEFs (M: molecular marker). **F**: Repeat of RT-PCR of RSK2−/− and RSK2+/+ MEFs shown in **E** to better separate the bands in agarose gel. **G**: Detection of mRSK4 variants in different mouse tissues, including a c-*myc* transgenic mammary tumor (mycMT). Note that the exon-24 deleted variants are detected faintly in the kidney and that the mRSK4 is more abundant in a c-*myc* pancreatic tumor (mycPT) than in normal pancreas.

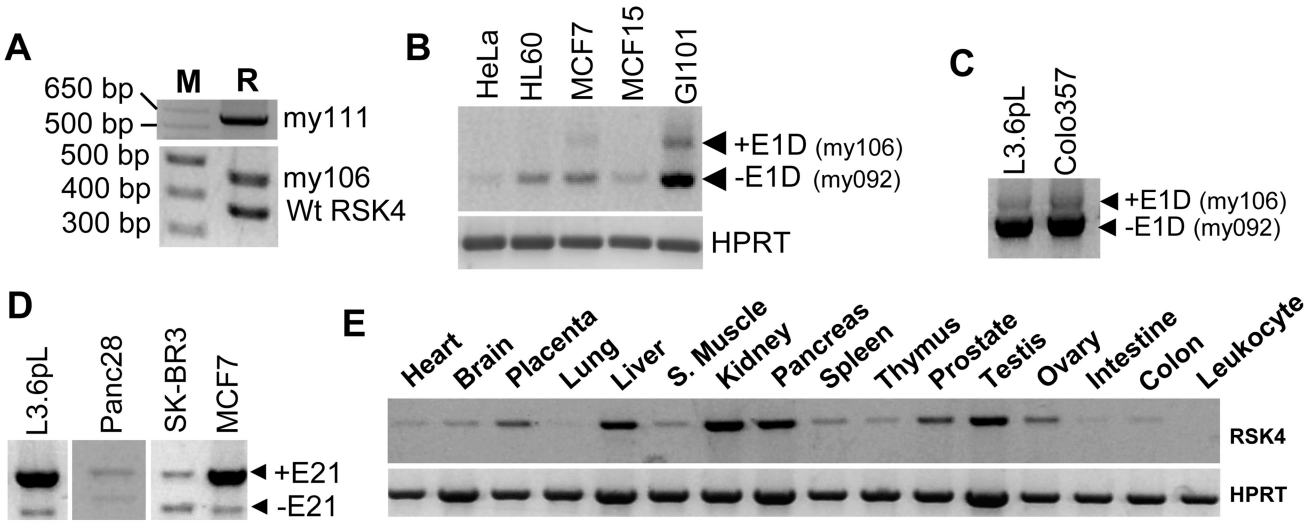

Fig. 3.

Expression of different hRSK4 variants. **A**: RT-PCR with the hF80+hR445 primers detects the my111 variant that contains E1B, E1C and E1D (depicted in S-Fig. 3A) and the my106 variant that contains E1D only (depicted in S-Fig. 3B), as well as their ratios to the NM_0144946.4 hRSK4 (wtRSK4), in a human brain cDNA library (M: molecular markers; R: RSK4). **B**: RT-PCR with the hF80+hR445 primers detects the my106 variant in GI101 and MCF7 cells. Note that RSK4 is hardly detected in Hela cells. **C**: RT-PCR with the hF80+mR1432 (equivalent to hR1018) primers also detects the my106 in L3.6pL and Colo357 cells. **D**: RT-PCR with the mF1912+mR2720 (equivalent to hF1457+hR2267) primers shows that the ratio between the ΔE21 variant and the intact hRSK4 varies among four human cell lines. **E**: RT-PCR detection of RSK4 in a panel of normal human organs with the same primers as in **D**. The liver seems to show a very faint band of the ΔE21 variant beneath the intact RSK4.

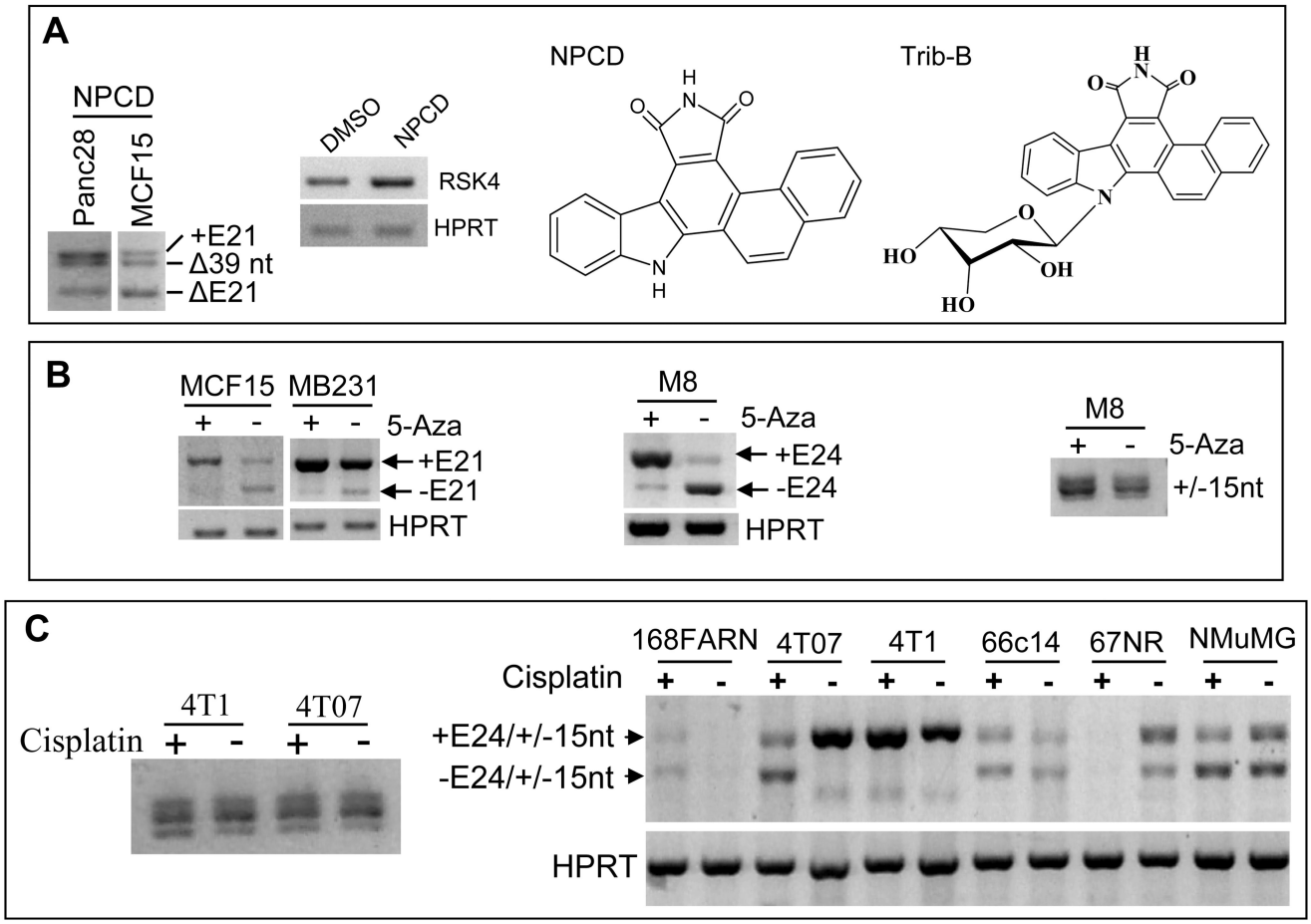

Fig. 4.

Effects of chemicals on RSK4 splicing. **A**: Treatment of Panc28 and MCF15 cells with indolocarbazole-derivatives NPCD and Trib-B, structures of which are shown, induces splicing at the 39th nt of exon 21, as detected by RT-PCR with the hF1791+mR2720 primers (1st panel), while the total hRSK4 mRNA level is slightly induced, compared with the treatment with the vehicle, DMSO (2nd panel). **B**: Treatment of the MCF15 and MB231 human cells (1st panel) as well as the M8 mouse cells (2nd panel) with 5-Aza decreases the level of the ΔE21 or ΔE24 variants while slightly increases the level of the intact RSK4. 5-Aza treatment does not affect the splicing at the 15th nt of E22 of mRSK4 (3rd panel). **C**: Treatment with cisplatin for two days does not obviously affect splicing at the 15th nt of E22 in 4T1 and 4T07 cells (left panel) but it affects the splicing at E24 in a manner that varies among 168FARN, 4T07, 4T1, 66C14, 67NR and NMuMG cells (right panel).

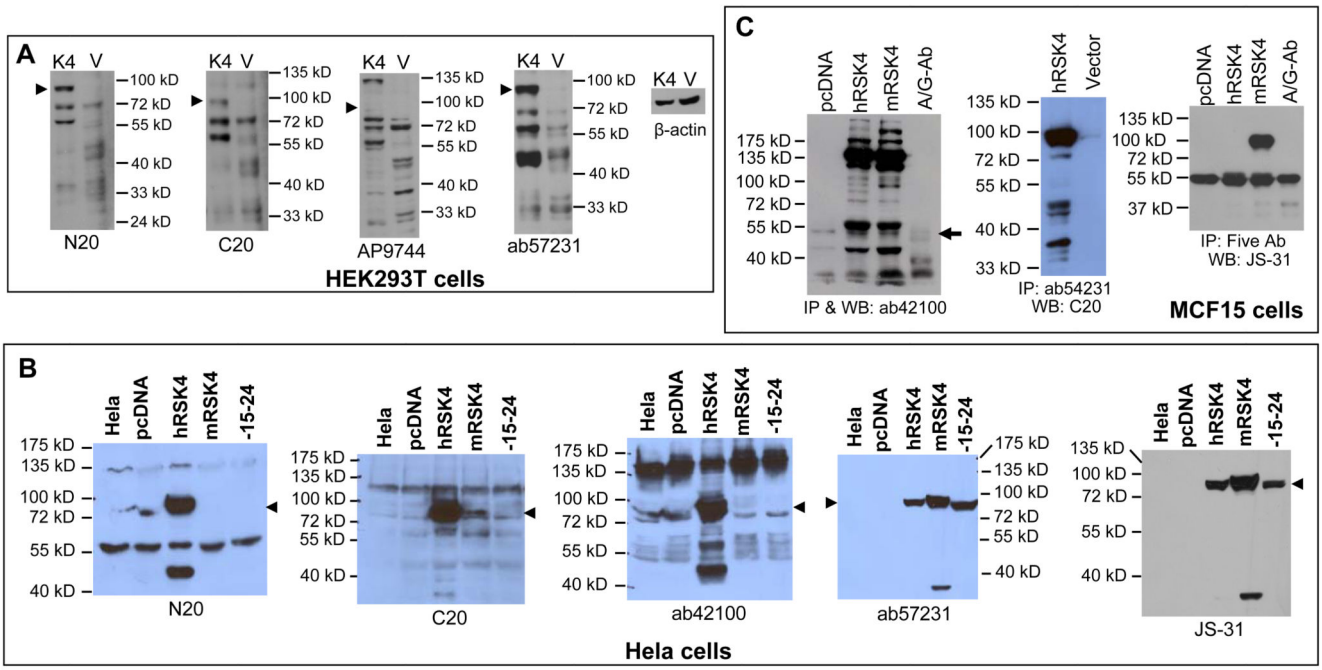

Fig. 5.

Determination of antibody specificity to the proteins expressed from cDNA. **A**: HEK293T cells were transfected with a pMIG vector (V) or the vector containing a hRSK4 cDNA (K4) starting from ATGβ. Western blot of the cell lysates using the indicated antibody detects multiple proteins at 90- (arrowhead), 72- and 55-kD that are much more abundant in the cDNA transfectants than in the vector counterpart, although the blot for β-actin shows that a less amount of protein from the cDNA transfectants was loaded. **B**: Transfection of Hela cells with the same hRSK4 cDNA in a pcDNA3.1 vector also results in multiple proteins detected by several antibodies, compared with non-transfected or vector-transfected Hela cells. Cells transfected with the intact mRSK4 that starts from ATGγ or with its Δ15ntΔE24 variant expressed the 90-kD (arrowhead) and a 37-kD proteins that were detected by ab57231 and JS-31 antibodies. **C**: MCF15 cells were transfected with the intact hRSK4 and the intact mRSK4 cDNA, with the empty pcDNA3.1 vector as control. Cell lysates were immunoprecipitated with one antibody as indicated (1st and 2nd panels) or with a cocktail of N20, C20, ab57231, ab42100 and JS-30 antibodies (3rd panel), followed by immunoblotting with the same or different antibody as indicated. Note that the 90-kD protein was precipitated in all three blots while multiple proteins were precipitated in the first two blots. Nonspecific immunoglobin and protein-A/G agarose beads, included as negative control, also pull down some 55-kD proteins (arrow).

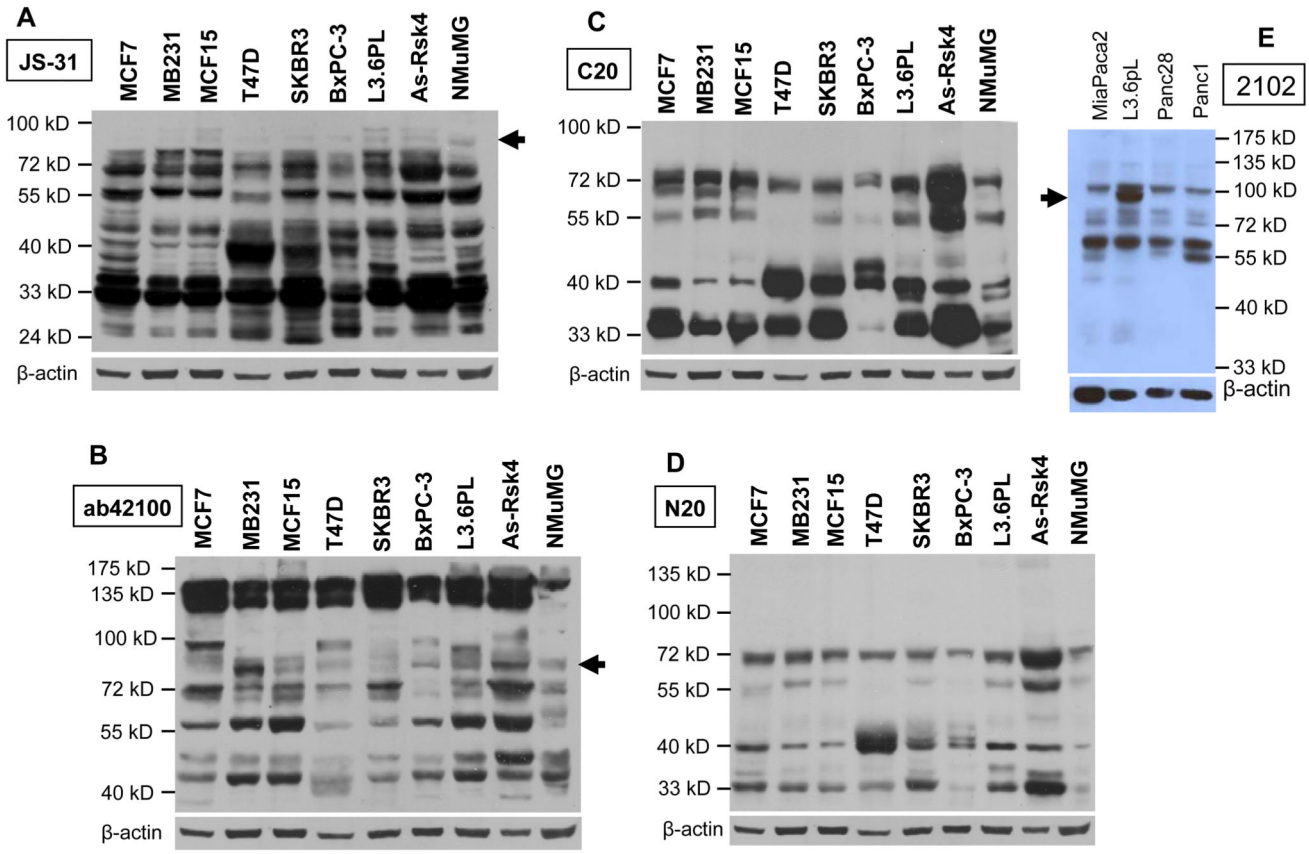

Fig. 6.

Determination of whether endogenous RSK4 proteins are detectable. Proteins from AsPC-1 cells transfected with the pMIG-hRSK4 construct were loaded at a less amount as a positive control. The proteins at 72- and 55-kD are the dominant ones and appear as duplet or triplet in most cell lines, as detected by most antibodies, whereas the putative wt hRSK4 proteins at 90-kD (arrow) is only detected by some antibodies, in some cell lines, or at such a low abundance that can be discerned only when the blots (**A** and **B**) were slightly overexposed. Some smaller proteins at about 48, 40 and 33 kD are also detected in some cell lines. The JS-31 antibody again shows high affinity to the proteins of mouse origin in NMuMG cells.

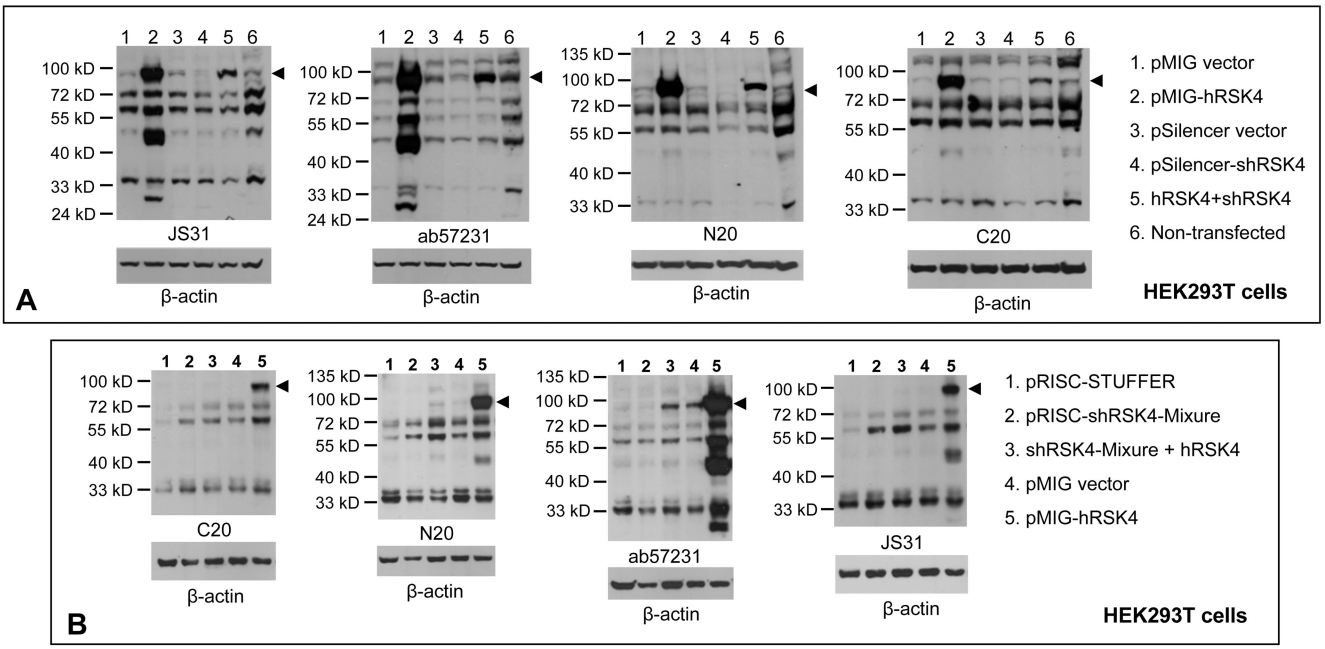

Fig. 7.

Verification of hRSK4 proteins with siRNA. **A**: HEK293T cells were transfected with an RSK4 shRNA in a pSilencer vector, alone or together with the pMIG-hRSK4 cDNA used in figure 5A. Controls include transfections with each empty vector and non-transfectants. Immunoblots with four different antibodies all show that the 90-kD protein (arrowhead) expressed from the hRSK4 cDNA is dramatically down regulated by the shRNA (lanes 2 *vs* 5), so as well the 48-kD protein. The 72- and 55-kD proteins are only partially decreased and the decrease is detected only by some of the four antibodies. **B**: HEK293T cells were transfected with the hSRK4 cDNA construct, alone or together with a mixture of five RSK4 shRNAs expressed from a pRISC-Stuffer vector.[17] Controls include cells transfected with each empty vectors. Immunoblots with indicated antibodies again show that the 90-kD protein is dramatically down regulated by the shRNA cocktail whereas the 72- and 55-kD proteins are only partially decreased (lanes 3 *vs* 5). After blotting with an RSK4 antibody, each membrane was stripped and then re-blotted with β-actin antibody to show the protein loading.

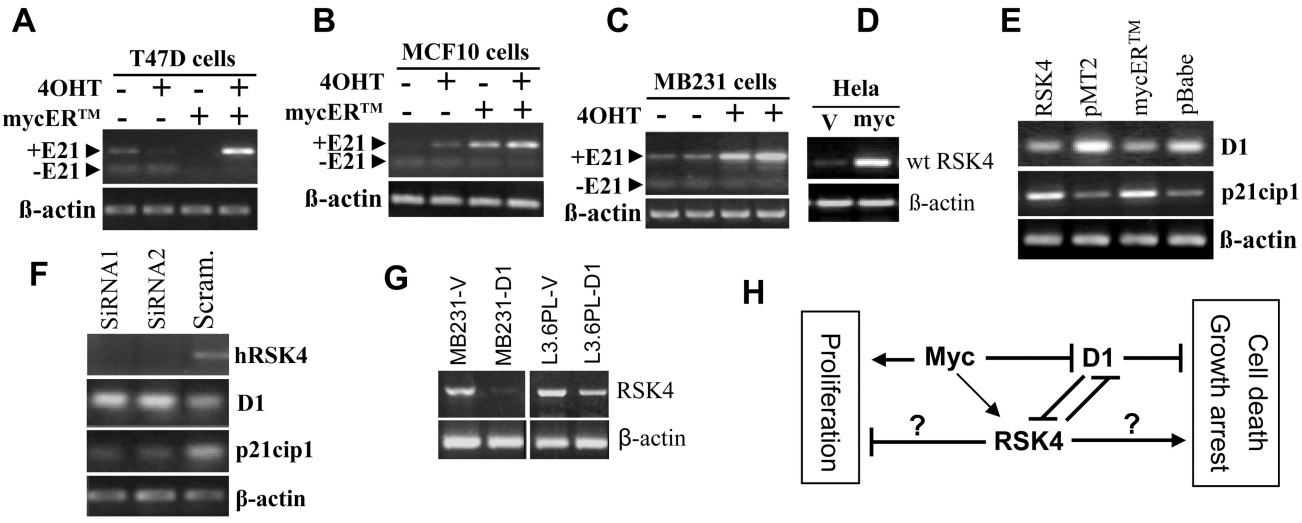

Fig. 8.

RT-PCR detection of mutual regulation among c-Myc, cyclin D1 (D1) and hRSK4. **A** and **B**: Transfection of T47D and MCF10 cells with a mycER™ construct followed by treatment with 4-hydroxyl-tamoxifen (4OHT) induces the intact hRSK4 mRNA, compared with the cells of various controls. In MCF10 cells the intact hRSK4 is slightly induced already, prior to 4OHT activation. The ΔE21 variant is not affected. **C**: In two separate experiments, 4OHT induces RSK4 mRNA without affecting the ΔE21 expression in the BM231 cells transfected with the mycER™ construct. **D**: Transfection of Hela cells with a c-*myc* cDNA[26] induces the intact RSK4 mRNA, compared to the transfection with the empty pcDNA3.1 vector (V). **E**: Transfection of Hela cells with an intact hRSK4 cDNA decreases the D1 mRNA level, compared to the transfection with the empty pMT2 vector. Similarly, transfection of Hela cells with the mycER™ construct followed by activation with 4-OHT also decreases D1 mRNA, compared with the cells transfected with the empty pBabe vector and treated with 4OHT. In these systems, the p21cip1 mRNA level shows the opposite change, i.e. induction by hRSK4 but inhibition by c-Myc activation. **F**: Transfection of T47D cells with two different RSK4 siRNA oligos, which decreases the RSK4 mRNA level, increases the D1 mRNA level but decreases the p21cip1 level, compared to transfection with a scrambled oligo. **G**: Transfection of MB231 and L3.6pL cells with a D1 cDNA decreases the intact hRSK4 mRNA level, compared to transfection with the pcDNA3.1 vector (V). **H**: Depiction of interactions among c-Myc, D1 and RSK4, with arrows, "⊣ ", and question mark representing stimulation, inhibition and uncertainty, respectively. c-Myc inhibits D1 but induces RSK4, whereas D1 and RSK4 inhibit each other. c-Myc is known for its dual effects, i.e. promotion of both cell proliferation and death, whereas D1 as a common sensor for many growth stimuli promotes cell proliferation and inhibits cell death,[30] in part by its inhibition of RSK4. Some RSK4 isoform(s) may inhibit cell proliferation and enhance growth arrest or cell death, but the actual effect depends on the dominant RSK4 isoform and other factors.

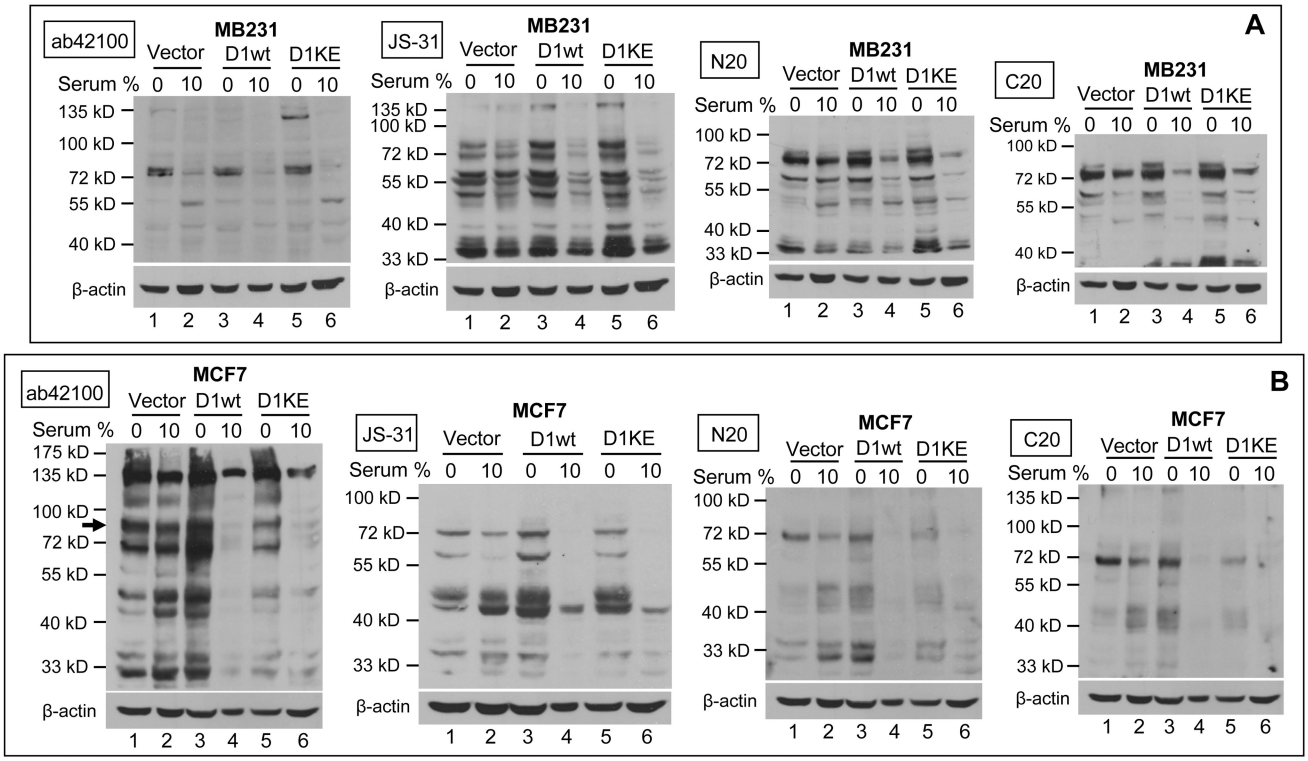

Fig. 9.

Effects of serum starvation and D1 on RSK4. MB231 (**A**) and MCF7 (**B**) cells sorted for a pMIG retrovirus that contains D1 or its K112E mutant were cultured in duplicate plates. One of the plates was then withdrawn from 10% serum for 48 hours. The cell lysates were immunoblotted with indicated antibodies and then were stripped and re-blotted with β-actin antibody to visualize the protein loading. Note that withdrawal of D1 or K112E expressing cells from serum increases the levels of most proteins detected by most antibodies, but the endogenous 90-kD protein is only detected in MCF7 cells by the ab42100 antibody (arrow).

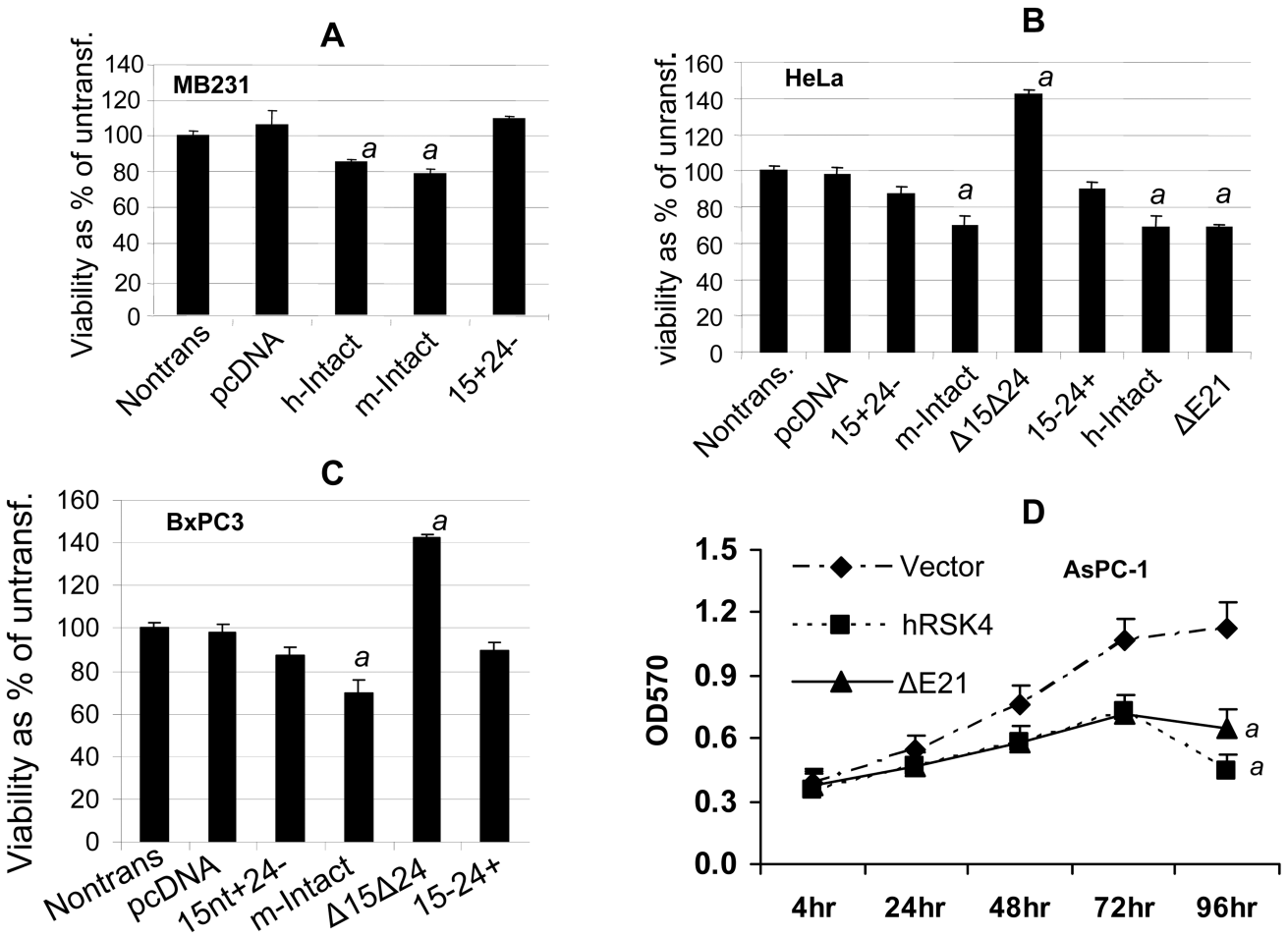

Fig. 10.

Effects of RSK4 on cell viability determined with MTT assay (mean ± SD). **A**, **B** and **C**: MB231, Hela and BxPC3 cells were transfected with cDNA of intact hRSK4, intact mRSK4, ΔE21/ΔE24, Δ15nt or Δ15ntΔE24 cloned into a pcDNA3.1 vector. MTT assay 72 hours later shows that the intact hRSK4 (h-Intact) or mRSK4 (m-Intact) slightly but significantly decreases, whereas the Δ15ntΔE24 increases, the number of viable cells, compared with non-transfected or vector-transfected (pcDNA) cells. Δ15 or ΔE24 did not show obvious effect compared with either the intact mRSK4 or the vector. ΔE21 has a similar effect with the intact hRSK4 in Hela cells. **D**: AsPC-1 cells sorted for a pMIG retrovirus that contains the intact hRSK4 or the ΔE21 show decreased viability at the 3rd and 4th days of culture, compared with the vector counterpart. *a*: significantly different from the vector counterpart ($p<0.05$).

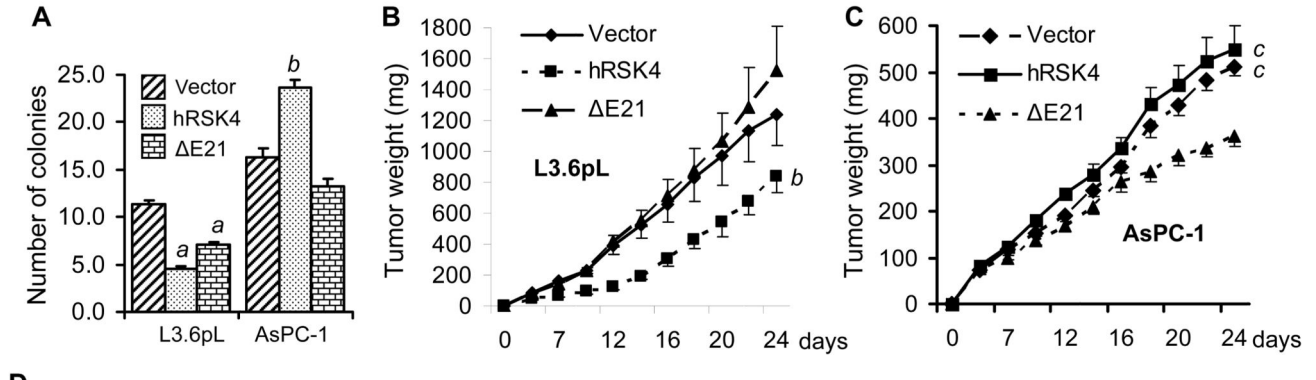

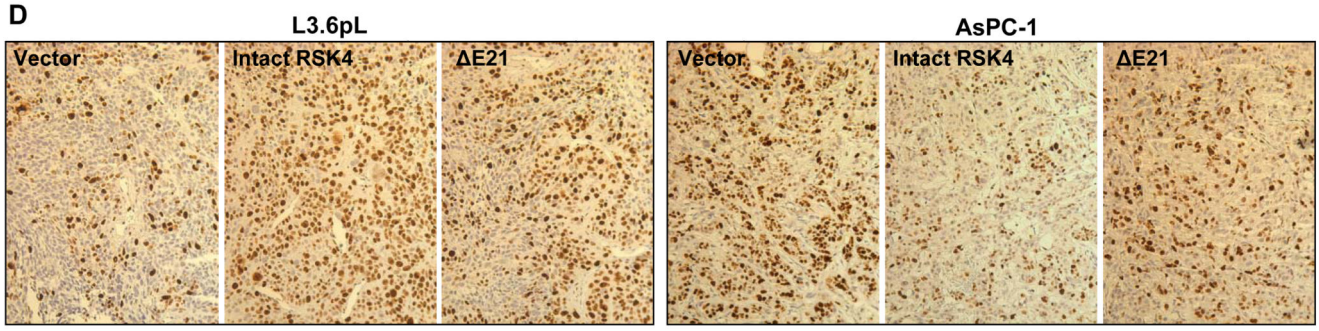

E

Percentages of proliferating cells, stroma and necrosis in exnograft tumors

	Ki-67			Stroma			Necrosis		
	Vector	Intact RSK4	ΔE21	Vector	Intact RSK4	ΔE21	Vector	Intact RSK4	ΔE21
L3.6pL	27±8%	77±7%^{b}	55±20%	33±4%	10±2%^{a}	11±3%^{a}	4±2%^{c}	5±1%^{c}	12±7%
AsPC-1	68±15%	25±7%^{b}	49±8%	15±3%	10±3%	20±6%	30±6%	54±9%^{b}	25±7%

Fig. 11.

Effects of RSK4 on colony formation in soft agar and on tumor growth in SCID mice. Data are presented as mean ± SD. L3.6pL and AsPC-1 cells sorted for the intact hRSK4- or ΔE21-containing pMIG retroviruses were seeded in soft agar or inoculated to SCID mice. **A**: The colony number of the intact hRSK4 or the ΔE21 expressing L3.6pL cells in soft agar is significantly less than that of the vector expressing cells. On the contrary, the AsPC-1 cells expressing the intact hRSK4 develop a larger number of colonies than the vector or the ΔE21-expressing cells. **B**: At the last two time points, the intact hRSK4 tumors of L3.6pL cells weigh less than the vector or the ΔE21 tumors. **C**: At the last two time points, the xenograft tumors of the intact-hRSK4 expressing AsPC-1 cells weigh similarly to the tumors of vector expressing cells but both are much larger than the ΔE21 tumors. **D**: Representative images of Ki-67 staining of the empty vector, the intact hRSK4, or the ΔE21 expressing L3.6pL and AsPC-1 xenograft tumors. **E**: Quantification of Ki-67 positive tumor cells as well as stromal and necrotic areas in L3.6pL and AsPC-1 xenograft tumors. *a*: significantly different from the vector counterpart ($p<0.05$); *b*: significantly different from both the vector and the ΔE21 counterparts ($p<0.05$); *c*: significantly different from the ΔE21 counterpart, which for the tumor size is at the last two days ($p<0.05$).

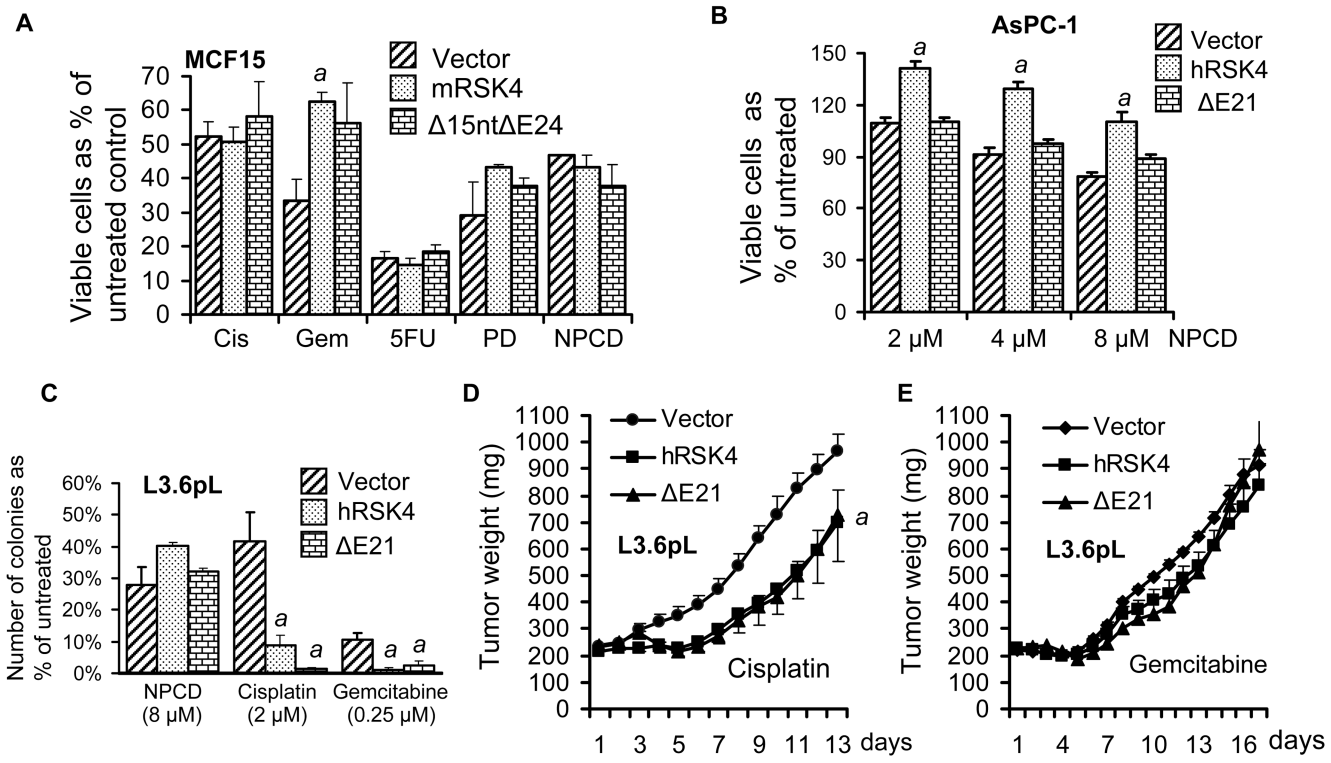

Fig. 12.

Effects of RSK4 on the response of cancer cells to chemotherapeutic agents. Data are presented as mean ± SD. **A**: In transfected MCF15 cells, MTT assay shows that the intact mRSK4 causes resistance to gemcitabine (Gem), relative to the pcDNA3.1 empty vector, whereas neither the intact mRSK4 nor its Δ15ntΔE24 variant affects the response to cisplatin (Cis), 5-fluorouracil (5-FU), PD0332991 (PD) or NPCD. **B**: In AsPC-1 cells sorted for different constructs, MTT assay shows that the intact hRSK4 increases the cell viability in response to escalating concentrations of NPCD. **C**: In L3.6pL cells sorted for different constructs, clonogenic survival assay shows that the intact hRSK4 and the ΔE21 decrease the number of cells that survive the treatment with cisplatin and gemcitabine, compared with the vector. **D** and **E**: SCID mice bearing xenograft tumors developed from sorted L3.6pL cells were treated with cisplatin (**D**) or gemcitabine (**E**). The intact hRSK4 tumors weigh similarly to the ΔE21 tumors but both are significantly smaller than the vector tumors in cisplatin treated mice. No difference is observed among the three groups treated with gemcitabine. *a*: significantly different from the vector counterpart, which for the tumor weights is calculated only for the last three days ($p<0.05$).

Table 1

Cell cycle distribution of BxPC3 cells transfected with mRSK4 variants

Plasmid	% in G1	% in S	% in G2-M	Total	% sub-G1
Vector	80.5±6.5	11.5±2.3	8.0±1.6	100	2.4±0.9
intact RSK4	82.5±9.0	10.1±2.8	7.4±2.0	100	10.6±1.8[a]
Δ15ntΔE24	72.7±8.0	18.5±1.9[a,b]	8.8±1.6	100	3.5±1.1
15ntΔE24	78.2±6.5	13.4±1.3	8.4±2.2	100	3.0±1.1
Δ15ntE24	80.2±8.8	13.4±2.1	8.4±1.4	100	4.1±1.3

Note: Data are presented as mean ± SD.

[a] significantly different from the vector transfected counterpart ($p<0.05$);

[b] significantly different from the intact RSK4 transfected counterpart ($p<0.05$).

Table 2

Effects of serum starvation on the cell cycle distribution of AsPC-1 cells

Time	Clone	%G1	% S	%G2-M	%subG1
24 hr	**Vector-0%**	70.95±4.6	22.67±4.25	6.38±1.98	0.79±0.23
	Vector-10%	25.91±6.11[a]	68.56±4.85[a]	5.53±1.66	1.34±0.58
	hRSK4-0%	51.55±8.81[c]	30.67±6.56[c]	17.78±2.36[c]	1.44±0.4
	hRSK4-10%	23.25±5.79[a,c]	62.99±4.8[a,c]	13.76±1.87[a,c]	2.29±0.29
	ΔE21-0%	43.47±2.13[c]	37.36±3.53[c]	19.17±2.0[c]	2.22±0.48
	ΔE21-10%	24.72±4.98[a]	71.04±6.27[a]	4.24±1.72[a,b]	2.73±0.6
48 hr	**Vector-0%**	75.33±4.5	18.71±3.21	5.96±1.55	1.54±0.62
	Vector-10%	31.99±2.19[a]	61.53±3.81[a]	6.48±1.03	2±0.46
	hRSK4-0%	53.61±4.04[c]	22.91±2.94[c]	23.48±2.45[c]	2.46±0.74
	hRSK4-10%	23.43±1.66[a,c]	58.21±1.89[a,c]	18.36±1.94[a,c]	2.51±0.37
	ΔE21-0%	45.68±3.11[c]	29.71±2.48[c]	24.62±1.63[c]	2.98±0.94
	ΔE21-10%	31.23±2.07[a]	62.56±2.15[a]	6.21±1.66[a,b]	2.61±0.43
72 hr	**Vector-0%**	79.98±3.81	13.54±2.15	6.48±2.0	1.73±0.76
	Vector-10%	33.57±1.02[a]	60.22±3.34[a]	6.21±0.34	2.33±0.54
	hRSK4-0%	54.48±1.56[c]	28.6±5.11[c]	16.92±1.56[c]	3.28±0.48
	hRSK4-10%	21.53±1.5[a,c]	61.1±3.13[a,c]	17.38±1.45[a,c]	1.44±0.59
	ΔE21-0%	45.11±0.9[c]	35.78±4.78[c]	19.11±1.0[c]	4.7[c]±0.58
	ΔE21-10%	30.86±1.45[a,b]	61.47±1.66[a]	7.66±1.67[a,b]	2.14±0.48
96 hr	**Vector-0%**	76.56±2.34	16.25±2.38	7.18±1.448	4.53±0.58
	Vector-10%	29.4±5.36[a]	63.77±2.33[a]	6.83±1.34	2.5±0.66
	hRSK4-0%	54.29±1.99[c]	29.59±2.25[c]	16.13±1.48[c]	6.24±0.38[c]
	hRSK4-10%	14.47±3.19[a,c]	70.92±2.28[a,c]	14.61±2.43[a,c]	2.17±0.8[a,c]
	ΔE21-0%	47.64±3.12[c]	34.95±1.86[c]	17.41±2.34[c]	7.31±0.65[c]

Time	Clone	%G1	% S	%G2-M	%subG1
	ΔE21-10%	29.44±1.01[a,b]	63.34±3.3[a]	7.22±1.41[a,b]	2.53±0.46[a]

Note: Data are presented as Mean ± SD. G1, S and G2 phase cells sum to 100% of viable cells. Sub-G1 are attached but dead cells.

[a] significantly different from 0% serum counterpart ($p<0.05$);

[b] significantly different from the intact hRSK4 counterpart ($p<0.05$);

[c] significantly different from the vector counterpart ($p<0.05$).